

445 | September 1984

SCHRIFTENREIHE SCHIFFBAU

Zhao Lian-en

**Optimal Ship Forms for Minimum
Total Resistance in Shallow Water**

TUHH

Technische Universität Hamburg-Harburg

Optimal Ship Forms for Minimum Total Resistance in Shallow Water

Zhao Lian-en, Hamburg, Technische Universität Hamburg-Harburg, 1984

© Technische Universität Hamburg-Harburg
Schriftenreihe Schiffbau
Schwarzenbergstraße 95c
D-21073 Hamburg

<http://www.tuhh.de/vss>

OPTIMAL SHIP FORMS FOR MINIMUM
TOTAL RESISTANCE IN SHALLOW WATER

by

Zhao Lian-en *)

Hamburg, September 1984

*) Harbin Shipbuilding Engineering Institute, Harbin, China, Visiting Scholar at Institut für Schiffbau, University of Hamburg, in the Summer of 1984.

TABLE OF CONTENTS

	Page
ABSTRACT	I
NOMENCLATURE	1
INTRODUCTION	3
FORMULATION OF THE PROBLEM	5
Expressions for Shallow-water Wave-Making Resistance	5
Expressions for Shallow-water Viscous Resistance	15
THE RESULTS OF CALCULATION	18
Calculation of Shallow-water Resistance and Comparison with Experimental Results	18
The Results of Optimization for Wave Resistance	21
The Results of Optimization for Total Resistance	29
CLOSING REMARKS	56
ACKNOWLEDGEMENT	58
REFERENCES	59

ABSTRACT

An attempt is made to obtain shallow-water optimal ship forms for total resistance by means of "tent" function representation under the constraints that the main dimensions of the ship and the water-line area were kept constant. The objective function in the quadratic programming is the sum of wave-making resistance calculated by Sretenski's formula and viscous resistance calculated by "1+k" form factor method. Thus, the present method can be used to obtain arbitrary-deep-water optimal ship forms for total resistance.

Under equal geometrical constraints the shallow-water optimal ship form is obviously different from the deep-water optimal ship form. It is felt that for shallow water the wave resistance is much more sensitive to the bow geometry than for deep water.

In the optimization process, it is shown that a practical optimal ship form, of which resistance performance was obviously improved, can be reached under a set of appropriate inequality-constraints.

NOMENCLATURE

A_o	:	constant determining the lower limit of unknown offsets
B_o	:	constant determining the higher limit of unknown offsets
c	:	velocity of ship or model
C	:	coefficient of linear term of object function
C_{Ro}	:	dimensionless wave-resistance coefficient before optimization
C_R	:	dimensionless wave-resistance coefficient after optimization
C_b	:	block coefficient of ship
C_p	:	prismatic coefficient of ship
C_{fo}	:	dimensionless frictional-resistance coefficient before optimization
C_f	:	dimensionless frictional-resistance coefficient after optimization
C_{to}	:	dimensionless total-resistance coefficient before optimization
C_t	:	dimensionless total-resistance coefficient after optimization
D	:	resistance matrix
$F(X,Z)$:	hull function
$f(x,z)$:	dimensionless hull function
g	:	acceleration of gravity
H	:	water depth
I,J	:	integrals over wetted surface of ship in Michell's integral
$\bar{I}, \bar{J}, I_1, J_1$:	corresponding expression of I, J in Sretenski's formula
$k = \mu H$:	dimensionless wave number
k	:	the form factor of ship
L_R	:	type number of unknown offset constraints
L	:	length of ship or model
p	:	the number of known offsets
q	:	the number of unknown offsets
P, Q	:	integrals over wetted surface of ship in Sretenski's formula

$\bar{P}, \bar{Q}, P_1, Q_1$:	corresponding expression of P, Q
R_f	:	frictional resistance
R_v	:	viscous resistance
R_w	:	wave resistance
S	:	wetted surface of ship
T	:	draft of ship
$u = \sqrt{\lambda - 1}$:	integration variable in wave resistance integral
X, Y, Z	:	coordinates in horizontal, transverse and vertical directions
x, y, z	:	corresponding dimensionless coordinates of X, Y, Z
V_D	:	change in Block coefficient after optimization
ζ_f	:	frictional resistance coefficient
$\lambda = 1/\cos$:	integration variable in Michell's integral
μ	:	wave number
$\nu = g/c^2$:	principal wave number
$F_n = c/\sqrt{gL}$:	Froude number
$F_h = c/\sqrt{gH}$:	depth Froude number

INTRODUCTION

Ship designers and hydrodynamicists have always been trying to find ship forms of minimum resistance. Various researchers so far have calculated ship forms of minimum wave resistance in deep water. In most cases, the variation was among a class of hull forms represented by closed forms mathematical expressions. C.C. Hsiung /1/** first considered arbitrary forms (which he approximated by "tent function") under application of linear programming.

The case of deep water is just a limiting case of the more general situation where the water depth is finite; in fact, Michell's wave resistance integral is a continuous limit of the finite depth expression derived by Sretenski.

The importance of considering finite depth effect for the ship resistance problem was emphasized in a concise but fundamental exposition by Graff, Kracht und Weinblum (1966): "... with the increase of ship speed, large parts of North Sea and coastal regions of Baltic Sea became shallow-water regions or regions of finite depth in the sense of resistance theory ..." /9/ This is also true in other coastal regions and inland waters.

The definition of "finite depth" may be best described by Saunders (1957): "A body of water is considered to be of 'finite depth' when the boundaries are close enough under the ship to affect its resistance, speed, attitude, manoeuvring, and other performance characteristics as compared to its corresponding behavior in a body of water of unlimited depth." /4/

It is difficult to separate finite-depth ship resistance into difference additive components. But for simplicity, the shallow-water ship resistance may be separated into parts due to friction and to wave-making as well. However, the value of both parts is distinct from that corresponding to deep water. When a ship moves in water of finite depth, the value of wave resistance varies both with F_n and the depth Froude number F_h .

** Number in brackets designate References at end of paper

In the light of the ship resistance characteristics of sidewise unrestricted water of finite depth, the ship speed generally may be divided into the following three different ranges:

1. $F_h < 0.6$. This may be described as "far subcritical speed range, at which there is no much difference between shallow water resistance and deep water resistance.
2. $F_h = 0.6 \sim 1.2$. This is known as near critical speed range and includes critical speed, at which shallow water resistance is much more greater than that in deep water. And shallow water wave resistance has maximum value at around critical depth Froude number $F_h = 1$ (see Fig. 1).
3. $F_h > \sim 1.2$. This can be called far supercritical speed range, at which shallow water resistance is rather smaller than that in deep water.

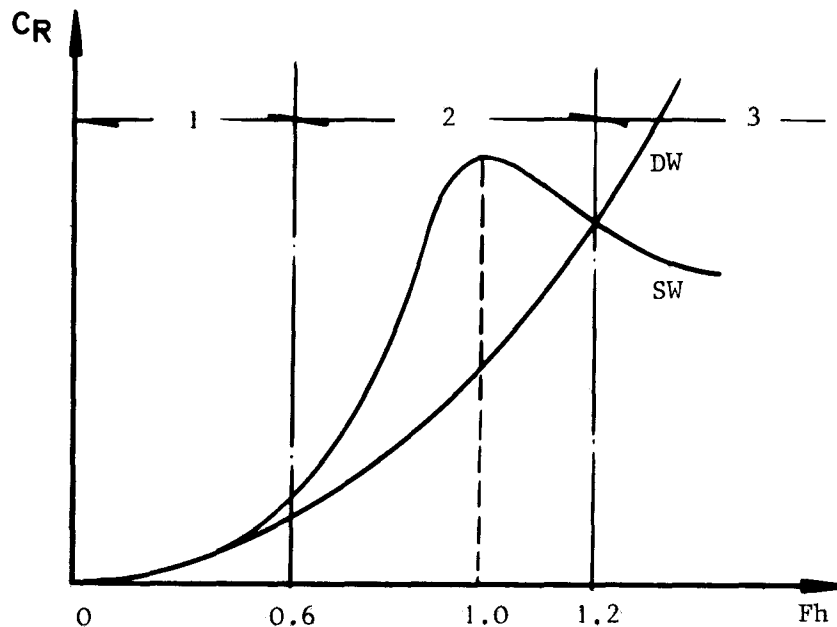


Figure 1

From Fig. 1, it is evident that in shallow water the importance of the wave portion of the ship's resistance increases, especially near the critical velocity $C_{cr} = \sqrt{gH}$, where H is the depth of the water. So there will even more be some sense in optimizing shallow-water ship forms on the basis of wave resistance.

FORMULATION OF THE PROBLEM

Expressions for Shallow Water Wave-Making Resistance

For a ship with a coordinate system complying with the conventional system for ship lines drawing as shown in Fig. 2, we may write Sretenski's formula for the wave resistance of a "thin" ship at constant speed C , draft T and depth of the water H in the following form /2//10/ :

$$R = \frac{2\rho g}{\pi} \int_{\mu_h}^{\infty} [P^2(\mu) + Q^2(\mu)] \sqrt{\frac{\mu}{\mu - v \tanh \mu \cdot H}} d\mu \quad \text{with} \quad (1-a)$$

$$\frac{P(\mu)}{Q(\mu)} = \iint_{S_0} F_x(X, Z) \frac{\cosh \mu(Z+H)}{\cosh \mu H} \frac{\cos}{\sin} (\kappa \sqrt{v \mu \tanh \mu H}) dX dZ$$

where $v = g/c^2$;

μ_h is the nonzero solution of $\mu = v \tanh \mu H$ if such exists, i.e. if $c^2/gH < 1$; otherwise $\mu_h = 0$. As $H \rightarrow \infty$, $\mu_h \rightarrow v$.

For numerical evaluation, the expressions for the wave resistance (1 - a) would be transformed so that the singularity at $\mu = \mu_h$ is eliminated in the integrand according to the dispersion relation of shallow-water waves

$$\mu \cos^2 \theta = v \tanh \mu H \quad (2)$$

one obtains

$$d\mu = \frac{2 \mu \cos \theta \sin \theta d\theta}{\operatorname{sech}^2 \mu H (\cos^2 \theta \cosh^2 \mu H - v H)} \quad (3)$$

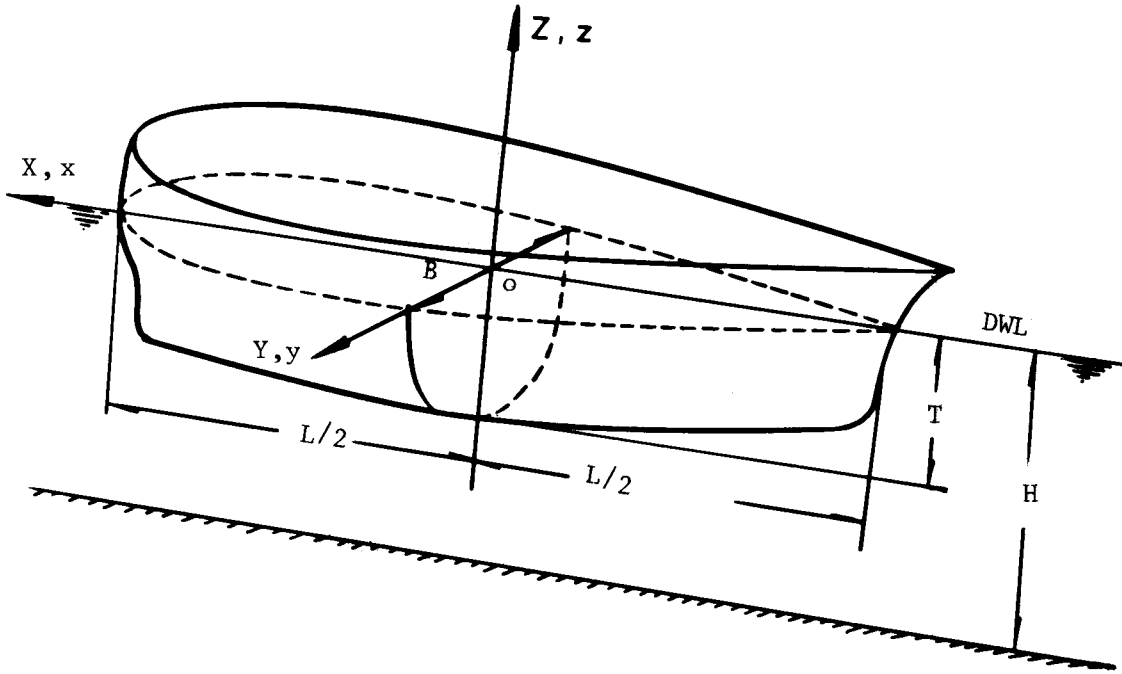


Figure 2

After substituting (3) into expression (1-a) and noticing the relation $\sin \theta = [(\mu - v \tanh \mu H) / \mu]^{1/2}$, we obtain the following formula for the shallow-water resistance R_w

$$R_w = \frac{4 \rho g^2}{\pi c^2} \int_{\theta_0}^{\pi/2} \frac{P_1^2(\theta) + Q_1^2(\theta)}{\operatorname{sech}^2 \bar{\mu} H} \frac{\tanh \bar{\mu} H \cdot \sec \theta}{\cos^2 \theta \cosh^2 \bar{\mu} H - vH} d\theta$$

with

(1-b)

$$\frac{P_1(\theta)}{Q_1(\theta)} = \iint_{S_0} F_x(X, Z) \frac{\cosh \bar{\mu}(Z+H)}{\cosh \bar{\mu} H} \frac{\cos}{\sin} (\chi \bar{\mu} \cos \theta) dX dZ$$

here $\theta_0 = 0$ if $vH > 1$; otherwise $\theta_0 = \arccos \sqrt{vH}$
with the new integration variable $\lambda = 1/\cos \theta$, then expression (1-b) becomes

$$R_w = \frac{4 \rho g^2}{\pi c^2} \int_{\lambda_h}^{\infty} [P^{-2}(\lambda) + Q^{-2}(\lambda)] \frac{\lambda^2 \tanh \bar{\mu} H (\lambda^2 - 1)^{-1/2}}{1 - \lambda^2 vH \operatorname{sech}^2 \bar{\mu} H} d\lambda$$

(1-c)

$$\frac{\bar{P}(\lambda)}{\bar{Q}(\lambda)} = \iint_{S_0} F_x(X, Z) \frac{\cosh \bar{\mu}(Z+H)}{\cosh \bar{\mu}H} \frac{\cos(\frac{\bar{\mu}}{\lambda} X)}{\sin(\frac{\bar{\mu}}{\lambda} X)} dX dZ$$

here $\lambda_h = 1$ if $F_h = c/\sqrt{gH} < 1$, and $\lambda_h = 1/\sqrt{vH}$ if $F_h > 1$
 $\bar{\mu}$ in (1-b) and (1-c) is the nonzero solution of the dispersion relation $\mu \cos^2 \theta = v \tanh \mu H$ is such exists (see Fig. 3).

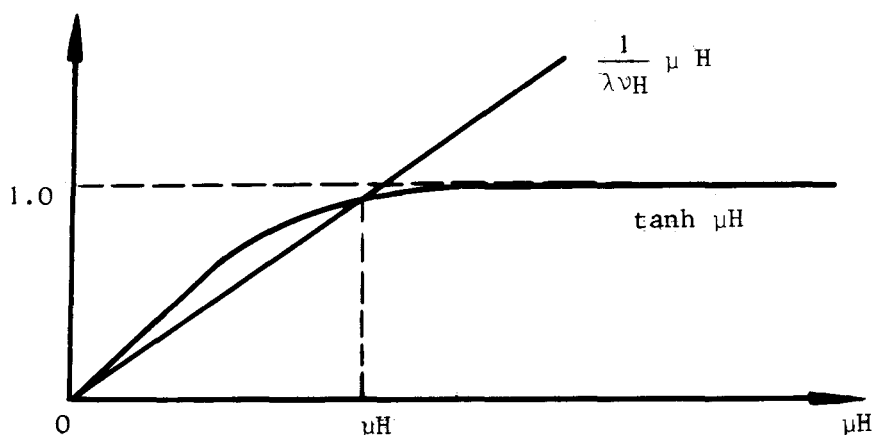


Figure 3

As $H \rightarrow \infty$, $\lambda_h \Rightarrow 1$ and one obtains one of the forms of Michell's integral:

$$Rw = \frac{4fg^2}{\pi c^2} \int_1^{\infty} (I^2 + J^2) \frac{\lambda^2}{\sqrt{\lambda^2 - 1}} d\lambda$$

with

(1 - d)

$$\begin{aligned} I(\lambda) &= \iint_{S_0} F_x(X, Z) e^{\lambda^2 v Z} \cos(\lambda v X) dX dZ \\ J(\lambda) &= \iint_{S_0} F_x(X, Z) e^{\lambda^2 v Z} \sin(\lambda v X) dX dZ \end{aligned}$$

It is evident that formula (1-a) can be used to calculate ship wave resistance in water of arbitrary depth.

After eliminating the singularity at $\lambda = 1$ by substituting $\lambda = u^2 + 1$, formula (1-c) becomes

$$R_w = \frac{8\rho g^2}{\pi c^2} \int_{u_h}^{\infty} [I_1^2(u) + J_1^2(u)] \frac{\bar{\mu}(u)}{1 - \lambda^2 v H \sec^2 h^2 \bar{\mu} H} \frac{1}{\sqrt{u^2 + 2}} du$$

with

(1-e)

$$I_1(u) = \iint_{S_0} F_x(X, Z) \frac{\cos h \bar{\mu}(z+H)}{\cos h \bar{\mu} H} \frac{\cos \left[\frac{\bar{\mu} u}{u^2+1} x \right]}{\sin \left[\frac{\bar{\mu} u}{u^2+1} x \right]} dX dZ$$

where $U_h = 0$ if $F_h < 1$, and $U_h = \sqrt{F_h - 1}$ if $F_h > 1$

Let $L, B=2b, T$ be respectively the length, beam and draft of ship. We introduce the following dimensionless variables:

$$\kappa = X/L, \quad y = Y/b, \quad z = Z/T \quad \text{and} \quad k = \mu H$$

Let $f(\kappa, z) = \frac{1}{b} F(X, Z)$ be the hull function; the slope function is

$$f_{\kappa}(\kappa, z) = \frac{L}{b} F_x(X, Z)$$

Then a dimensionless shallow-water wave resistance coefficient for the depth Froude number F_n , draft-depth ratio T/H and length-depth ratio L/H can be written as

$$C_R = R_w / \frac{8\rho g}{\pi} \frac{B^2 T^2}{L}$$

$$= \frac{1}{4} \left(\frac{L}{H} \right) \int_{U_h}^{\infty} \frac{\bar{k} F_n^2 (u^2 + 2)^{-\frac{1}{2}}}{F_h^2 - (u^2 + 1)^2 \sec^2 h^2 \bar{k}} (\bar{I}^2 + \bar{J}^2) du$$

with

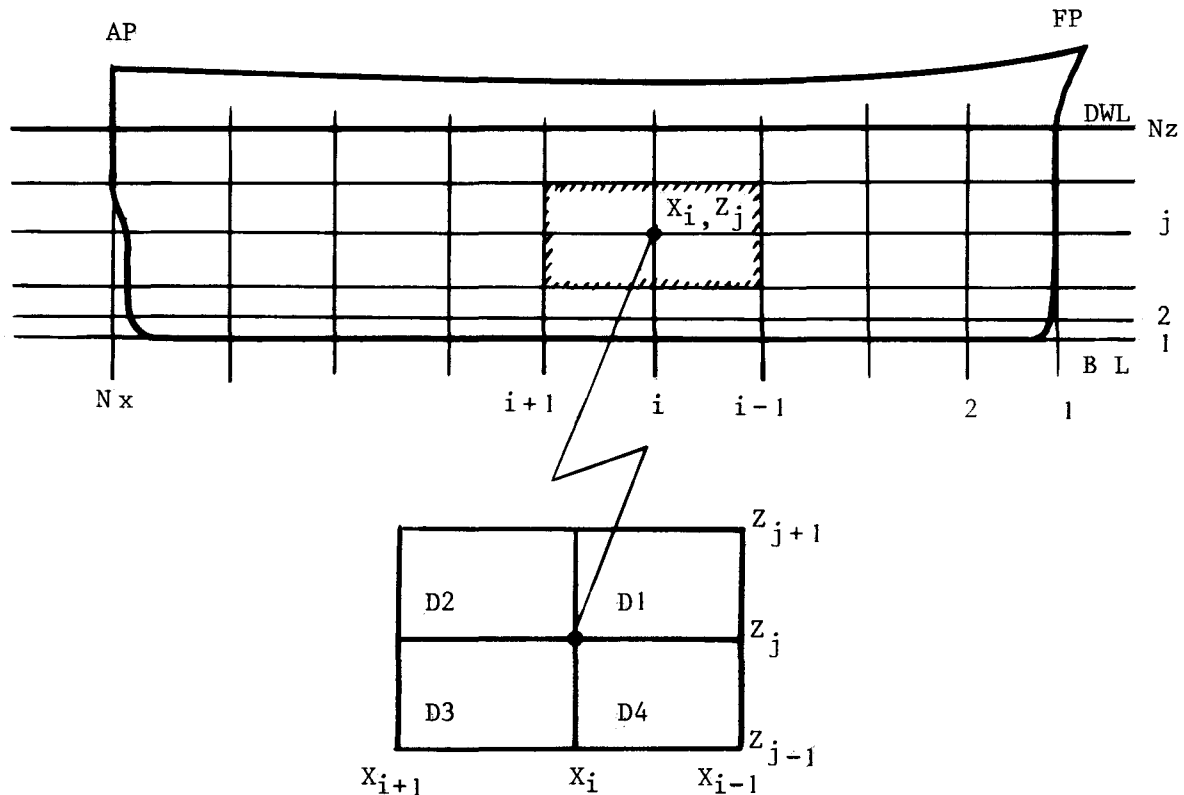
(1-f)

$$\frac{\bar{I}(u)}{\bar{J}(u)} = \int_{-1}^{0/2} \int_{-1/2}^{1/2} f_{\chi}(\chi, z) \frac{\cosh \bar{k} (1 + \frac{I}{H} z)}{\cosh \bar{k}} \cos \left[\frac{k}{u^2 + 1} \cdot \frac{L}{H} \chi \right] d\chi dz$$

here $U_h = 0$ if $F_h < 1$; otherwise $U_h = \sqrt{F_h - 1}$

\bar{k} is the nonzero solution of the dimensionless dispersion relation $k/\lambda^2 = \text{th } k/F_h^2$ if such exists.

As usual, a ship hull can be divided into a finite number N_x of stations (including the mostforward point and the aftermost point) and N_z waterlines (including the base-line and the design waterline) as shown as in Fig. 4.



Stations: $i=1, 2, \dots, N_x$; Waterlines: $j=1, 2, \dots, N_z$.

Figure 4

In the rectangular element D centered at grid point (κ_j, z_j) , as shown in Fig. 4, we use a unit "tent" function /1/ as following;

$$\begin{aligned}
 h^{(i,j)}(\kappa, z) \equiv & \left. \begin{aligned}
 & \left[\frac{\kappa - \kappa_{i+1}}{\kappa_i - \kappa_{i+1}} \right] \left[\frac{z - z_{j+1}}{z_j - z_{j+1}} \right], & (\kappa, z) \in D1 \\
 & \left[\frac{\kappa - \kappa_{i-1}}{\kappa_i - \kappa_{i-1}} \right] \left[\frac{z - z_{j+1}}{z_j - z_{j+1}} \right], & (\kappa, z) \in D2 \\
 & \left[\frac{\kappa - \kappa_{i-1}}{\kappa_i - \kappa_{i-1}} \right] \left[\frac{z - z_{j-1}}{z_j - z_{j-1}} \right], & (\kappa, z) \in D3 \\
 & \left[\frac{\kappa - \kappa_{i+1}}{\kappa_i - \kappa_{i+1}} \right] \left[\frac{z - z_{j-1}}{z_j - z_{j-1}} \right], & (\kappa, z) \in D4 \\
 & 0, & \text{elsewhere} & (\kappa, z) \notin D
 \end{aligned} \right\} \quad (4)
 \end{aligned}$$

here $D = D1 \cup D2 \cup D3 \cup D4$

The family of "tent" functions will now be used to construct a function approximating the hull surface. If y_{ij} is the hull offset at point (κ_i, z_j) , the approximation function is defined the following:

$$f(\kappa, z) = \sum_i \sum_j y_{ij} h^{(i,j)}(\kappa, z) \quad (5)$$

with "tent" function, formula (1-f) can be reduce to much simpler form. Substituting (5) into (1-f), we are led to introduce functions C_i, S_i and E_j :

$$\begin{aligned}
C_i &= \int_{\alpha_{i-1}}^{\alpha_i} \frac{\cos\left(\frac{k}{\lambda} \frac{L}{H} \cdot \alpha\right)}{\alpha_i - \alpha_{i-1}} d\alpha \\
&\quad + \int_{\alpha_i}^{\alpha_{i+1}} \frac{\cos\left(\frac{k}{\lambda} \frac{L}{H} \cdot \alpha\right)}{\alpha_i - \alpha_{i+1}} d\alpha \\
&= \frac{1}{a} \left[\frac{1}{\alpha_i - \alpha_{i-1}} (\sin a \alpha_i - \sin a \alpha_{i-1}) \right. \\
&\quad \left. - \frac{1}{\alpha_{i+1} - \alpha_i} (\sin a \alpha_{i+1} - \sin a \alpha_i) \right] \quad (6)
\end{aligned}$$

here $a = \frac{k}{\lambda} \frac{L}{H}$

$$\begin{aligned}
S_i &= \int_{\alpha_{i-1}}^{\alpha_i} \frac{\sin a \alpha}{\alpha_i - \alpha_{i-1}} d\alpha \\
&\quad + \int_{\alpha_i}^{\alpha_{i+1}} \frac{\sin a \alpha}{\alpha_i - \alpha_{i+1}} d\alpha \\
&= \frac{1}{a} \left[- \frac{1}{\alpha_i - \alpha_{i-1}} (\cos a \alpha_i - \cos a \alpha_{i-1}) \right. \\
&\quad \left. + \frac{1}{\alpha_{i+1} - \alpha_i} (\cos a \alpha_{i+1} - \cos a \alpha_i) \right] \\
E_j &= \int_{z_{j-1}}^{z_j} \frac{z - z_{j-1}}{z_j - z_{j-1}} \frac{\cosh k \left(1 + \frac{T}{H} z\right)}{\cosh k} dz \\
&\quad + \int_{z_j}^{z_{j+1}} \frac{z - z_{j+1}}{z_j - z_{j+1}} \frac{\cosh k \left(1 + \frac{T}{H} z\right)}{\cosh k} dz \quad (7) \\
&= -\frac{1}{b} \sinh(k + bz_j) + \frac{1}{b^2 (z_{j+1} - z_j)} \left[\frac{\cosh(k + az_{j+1}) - \cosh(k + az_j)}{\cosh k} \right] \\
&\quad + \frac{1}{b} \sinh(k + bz_j) - \frac{1}{b^2 (z_j - z_{j-1})} \left[\frac{\cosh(k + az_j) - \cosh(k + az_{j-1})}{\cosh k} dz \right]
\end{aligned}$$

here $b = \frac{k}{H} T$ (8)

Then with (6), (7) and (8), we obtain

$$\begin{aligned} \bar{I} = \sum_i \sum_j y_{ij} & \left\{ \left[\int_{\alpha_{i-1}}^{\alpha_i} \frac{\cos\left(\frac{k}{\lambda} \frac{L}{H} \alpha\right)}{\alpha_i - \alpha_{i-1}} d\alpha \right. \right. \\ & + \left. \int_{\alpha_i}^{\alpha_{i+1}} \frac{\cos\left(\frac{k}{\lambda} \frac{L}{H} \alpha\right)}{\alpha_i - \alpha_{i+1}} d\alpha \right] \times \\ & \left[\int_{z_{j-1}}^{z_j} \frac{z - z_{j-1}}{z_j - z_{j-1}} \frac{\cosh k\left(1 + \frac{T}{H} z\right)}{\cosh k} dz \right. \\ & \left. \left. + \int_{z_j}^{z_{j+1}} \frac{z - z_{j+1}}{z_j - z_{j+1}} \frac{\cosh k\left(1 + \frac{T}{H} z\right)}{\cosh k} dz \right] \right\} \\ & = \sum_i \sum_j y_{ij} \cdot C_i \cdot E_j \end{aligned}$$

Similarly,

$$\bar{J} = \sum_i \sum_j y_{ij} S_i E_j$$

Furthermore

$$\left. \begin{aligned} \bar{I}^2 &= \sum_{i,j} \sum_{k,l} y_{ij} y_{kl} C_i C_k E_j E_l \\ \bar{J}^2 &= \sum_{i,j} \sum_{k,l} y_{ij} y_{kl} S_i S_k E_j E_l \end{aligned} \right\} \quad (9)$$

Substituting (9) into (1-f), we obtain

$$\begin{aligned} C_R &= \sum_{i,j} \sum_{k,l} y_{ij} y_{kl} \frac{L}{4H} \int_{U_h}^{\infty} \frac{k F_h^2 (C_i C_k + S_i S_k)}{\left[F_h^2 - \frac{(U^2+1)^2}{\cosh k} \right] \sqrt{U^2+2}} E_j E_l dU \\ &= \sum_{i,j} \sum_{k,l} y_{ij} y_{kl} d_{ijkl} (F_h, L/H, T/H) \end{aligned} \quad (10)$$

where

$$d_{ijkl} (F_h, L/H, T/H) = \frac{L}{4H} \int_{U_h}^{\infty} \frac{k F_h^2 (C_i C_k + S_i S_k)}{\left[F_h^2 - \frac{(U^2+1)^2}{\cosh k} \right] \sqrt{U^2+2}} E_j E_l dU$$

which is independent of ship offsets and depends only on the depth Froude number F_h , length-depth ratio L/H and draft-depth ratio T/H .

We are able to write formula (10) in the following quadratic form

$$C_R = \sum_{m=1}^{\bar{m}} \sum_{n=1}^{\bar{m}} d_{mn} y_m y_n \quad (11)$$

where

$$m = i + (j - 1) \cdot N_x,$$

$$n = k + (l - 1) \cdot N_x,$$

$$\bar{m} = N_x \cdot N_z.$$

N_x, N_z and \bar{m} are respectively the summation limit of $i(k), j(l),$ and $m(n).$

Formula (11) can also be written in the following matrix form

$$CR = \mathbf{y}^T \cdot \mathbf{D} \cdot \mathbf{y} \tag{12}$$

where

\mathbf{y} = column \bar{m} -vector of offsets

\mathbf{y}^T = transpose of \mathbf{y}

\mathbf{D} = $\bar{m} \cdot \bar{m}$ resistance matrix

Observing that in general there will be more symmetries in the matrix \mathbf{D} besides the obvious relation $d_{mn} = d_{nm}$ we can reduce a large amount of calculation /11/.

Expressions for shallow-water Viscous Resistance

In the present study the viscous resistance R_v is expressed as the sum of the frictional resistance R_f and the viscous pressure resistance R_{vp} i.e.

$$\begin{aligned} R_v &= R_f + R_{vp} \\ &= (1+K) R_f \end{aligned}$$

here $K = R_{vp}/R_f$ is the form factor, which for deep water, say for $F_h \leq 0.35$, was given by F. Horn /4/, as follows

$$\begin{aligned} K &= 0.01 \left[\frac{(11,25 - L/B)^2}{5} + 2,5 \right] \times \\ &\quad (0,35 + C_p) \left(1,3 - \frac{B/T}{10} \right) \end{aligned} \tag{13}$$

For shallow water the form factor was given from experimental materials /14/ as

$$\begin{aligned} K &= -0.03397 H/T \times L/B + 0.0038524 L/B \times B/T \\ &\quad - 0.0013 (H/T)^3 + 0.00468 (H/T)^2 \times L/B \\ &\quad + 0.3755 \end{aligned}$$

for shallow water and $F_h \leq 1.0$ (14)

The frictional resistance is taken as proportional to the wetted surface area of ship, i.e.

$$R_f = \frac{1}{2} \rho C^2 S \zeta_f (Rn) \tag{15}$$

And the wetted surface area of the hull can be computed by the following approximated form /3/ :

$$S = 2 \iint_{S_0} \left(1 + \frac{1}{2} F_x^2 + \frac{1}{2} F_z^2 \right) dX dZ \tag{16}$$

The same non-dimensional dealing as above would have led us to the following expression:

$$S = 2LT \int_{-1/2}^{1/2} \int_{-1}^0 \left(1 + \frac{1}{8} \frac{B^2}{L^2} f_x^2 + \frac{1}{8} \frac{B^2}{T^2} f_z^2 \right) dx dz \quad (17)$$

Applying the "tent" function to the expression, we have the following form:

$$S = 2LT \int_{-1/2}^{1/2} \int_{-1}^0 \left[\left(1 + \frac{1}{8} \frac{B^2}{L^2} h_x(\chi, J) + \frac{1}{8} \frac{B^2}{T^2} h_z^2(\chi, z) \right) \right] dx dz \quad (18)$$

It follows from the detailed derivations in the paper /7/ that formula (18) can be expressed in the following form:

$$S = C_{S_0} + \mathbf{C}_S^T \cdot \mathbf{y} + \mathbf{y}^T \cdot \mathbf{A}_S \mathbf{y} \quad (19)$$

where

- C_{S_0} = constant term
- \mathbf{C}_S = coefficient column-vector of linear term
- \mathbf{A}_S = surface area matrix

Adopting ITTC (1957) formula for the frictional resistance line, the frictional resistance coefficient is:

$$\zeta_f = 0.075 / (\log_{10} - Rn - 2)^2 \quad (20)$$

For consistency with the definition of the wave resistance coefficient (1-f), we also have corresponding form

$$\begin{aligned} C_f &= R_f / \left(\frac{8 \rho g}{\pi} \frac{B^2 T^2}{L} \right) \\ &= \zeta_f F_n^2 S / \left[\frac{16}{\pi} \left(\frac{BT}{L} \right)^2 \right] \end{aligned} \quad (21)$$

Substituting (19) into (21), the frictional resistance of ship can be written in the following form:

$$C_f = C_{F_0} + \mathbf{C}_{FL}^T \cdot \mathbf{y} + \mathbf{y}^T \cdot \mathbf{A}_F \mathbf{y} \quad (22)$$

Combining with the wave resistance coefficient (22) and taking the form factor K into account, we obtain the total ship resistance coefficient as the following:

$$\begin{aligned} C_T &= C_W + (1+K) C_f \\ &= C_{T_0} + \mathbf{C}_{TL}^T \cdot \mathbf{y} + \frac{1}{2} \mathbf{y}^T \cdot \mathbf{D}_T \cdot \mathbf{y} \end{aligned} \quad (23)$$

It is evident that optimization problem of formula (23) becomes the following convex quadratic programming problem:

minimize

$$\left. \begin{aligned} & \mathbf{C}_{TL}^T \cdot \mathbf{y} + \frac{1}{2} \mathbf{y}^T \cdot \mathbf{D}_T \cdot \mathbf{y} \\ \text{Subject to} & \\ & \mathbf{A} \cdot \mathbf{y} \geq \mathbf{b}, \mathbf{y} \geq \mathbf{0} \end{aligned} \right\} \quad (24)$$

(24) can be solved by means of C.E. Lemke's algorithm which is based on the "Complementary Pivot Scheme" /8//12/ .

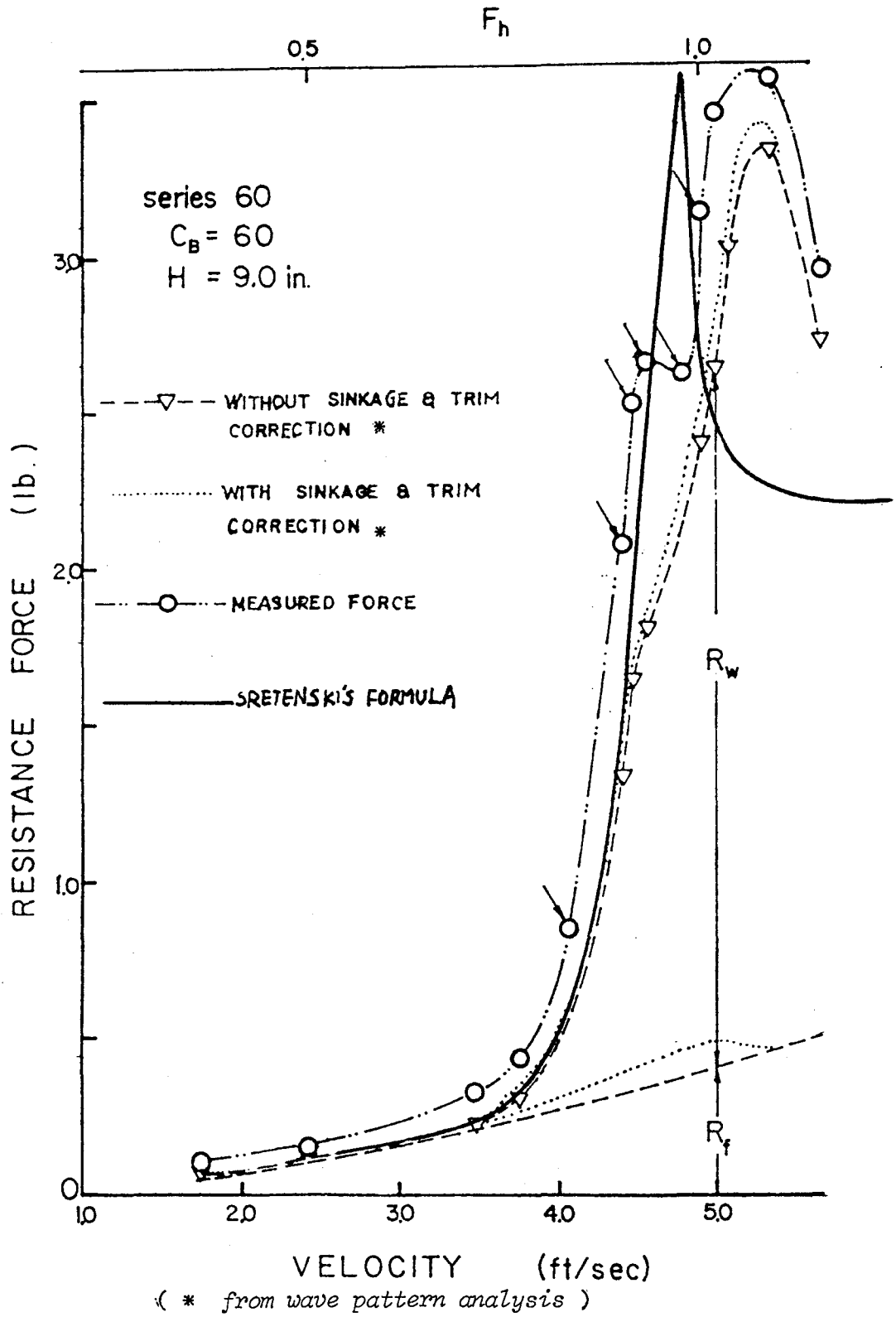
THE RESULTS OF CALCULATION

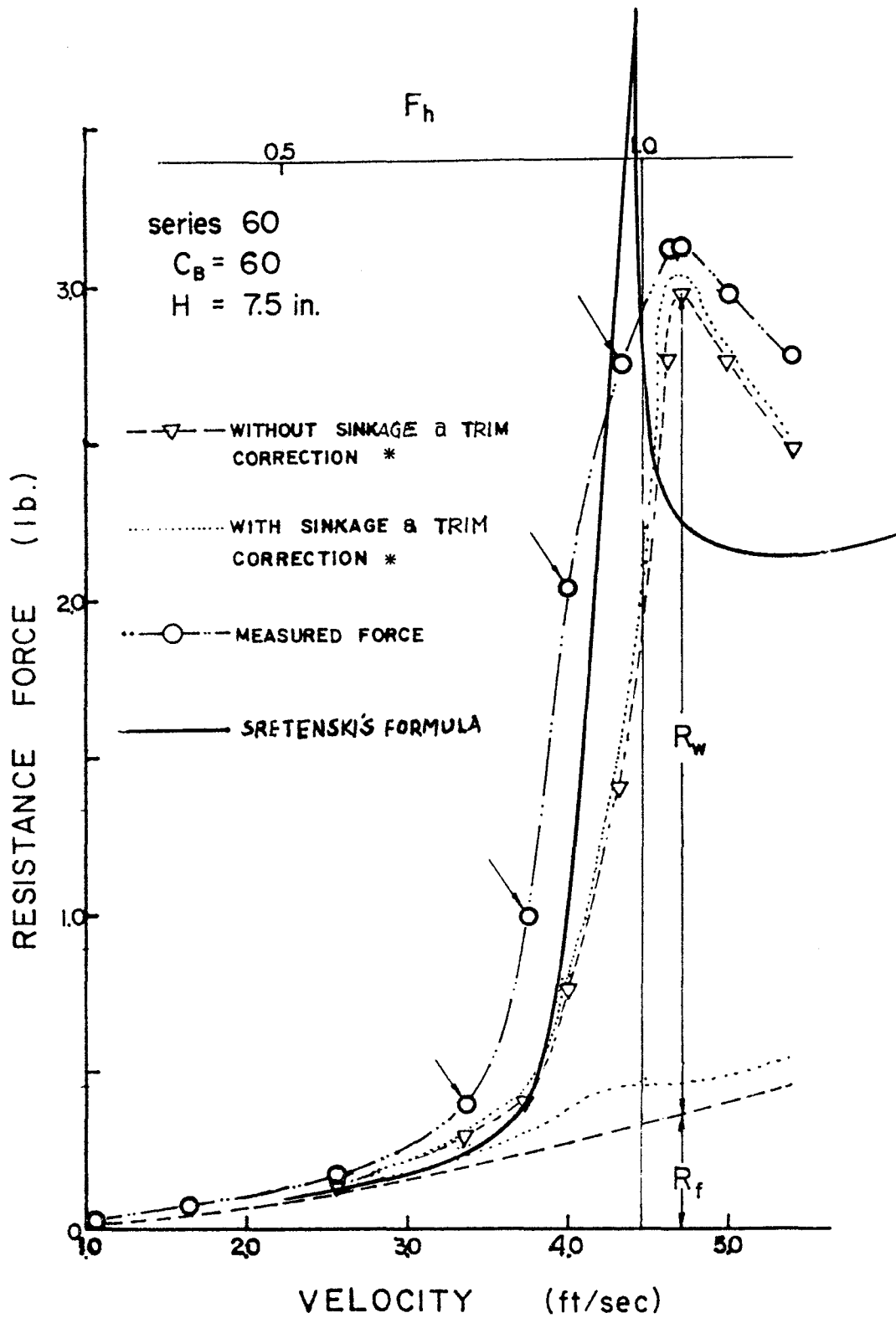
Calculation of Shallow-water Resistance and Comparison with Experimental Results

As pointed out previously, Sretenski's formula (1-a) can be used to calculate wave resistance of both shallow water and deep water. Before optimizing ship forms the computation of wave resistance was carried out to compare with the results from the experiments which were made by Kenneth Keh-ya Chen /5/. The test model was a 5-foot model of Series 60, Block 60. The overall dimensions of the model basin are 149.5 ft. long by 63.6 ft. wide and 2.5 ft. deep. It is evident that the effect of tank walls on the wave resistance can be neglected. For this reason, the body of water can be considered to be "side-wise" unrestricted water of finite depth.

We computed the wave resistance of Series 60, Block 60 model for the same depth of water as in Chen's paper. Our computational results were plotted in the same figures which were taken from reference /5/, shown in Figure 5 and 6. There were two curves in Chen's picture: one based on his measurement, and the other based on wave pattern analysis. From Figures 5 and 6, one sees that the curves from Sretenski's formula has the same tendency as those from experiments.

The calculation of wave resistance coefficient of Series 60, Block 60 had also been carried out for keeping Froude number $F_n = 0.289$ to be constant. The results were plotted against depth Froude number F_h in figure 7. Here we can see the effect of water depth on wave resistance at the given Froude number, and it is evident that when depth Froude number $F_h < 0.6$, there is no much difference between shallow-water resistance and deep-water resistance.





(* from wave pattern analysis)

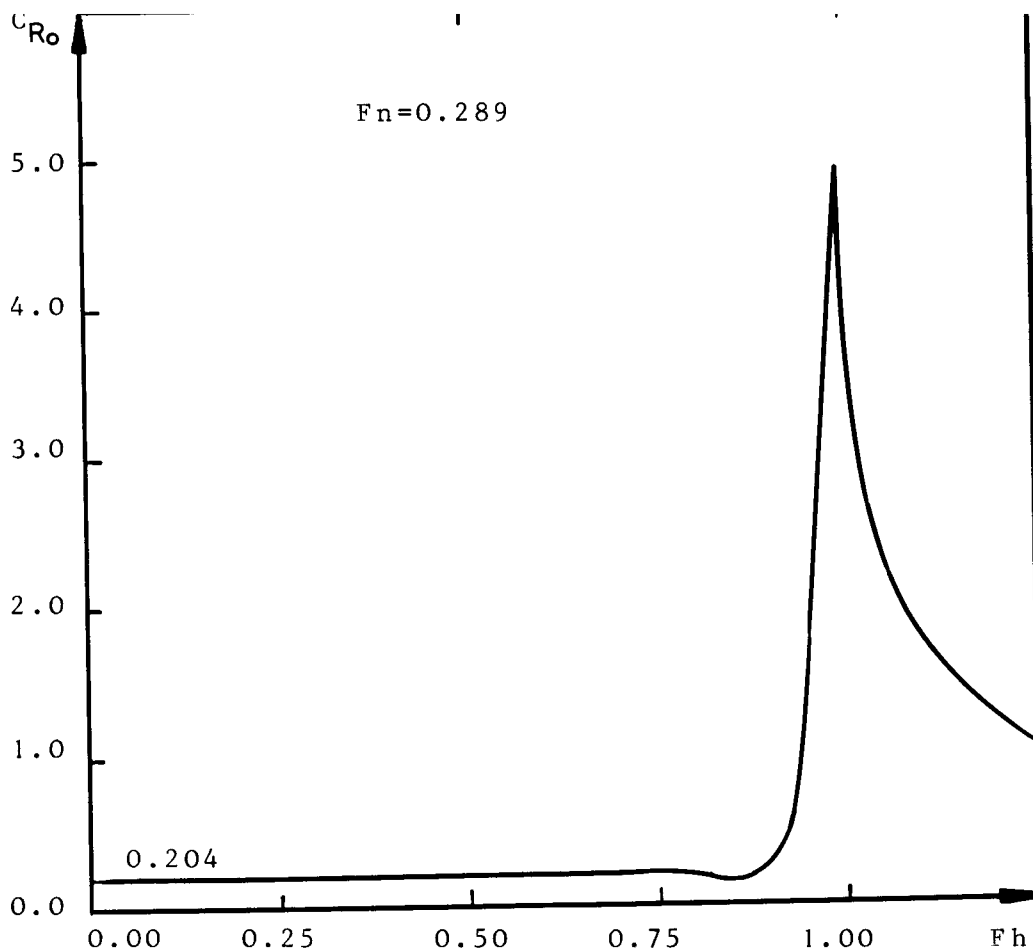


Figure 7

The Results of Optimization for Wave Resistance

As stated above, the problem of finding the optimal ship forms for minimum wave resistance based on the thin-ship theory can be solved by using C.E. Lemke's Complementary Pivot Scheme. In order to check the programming of computation, we first calculated a mathematical model $y = (1-x)(1-z)$, which was under the same conditions as that in Hsiung's paper /1/, i.e., the draft length ratio of the model was taken as $T/L = 0.1$, Froude number $F_n = 0.316$, and all offsets fixed at the values given by the above equation except for station 2. The results of the present calculation, which subject to the constraints $y_{2j} \leq 0$ and $0 \leq y_{2j} \leq 1$, are shown in Fig. 8(a) and 9(a) respectively.

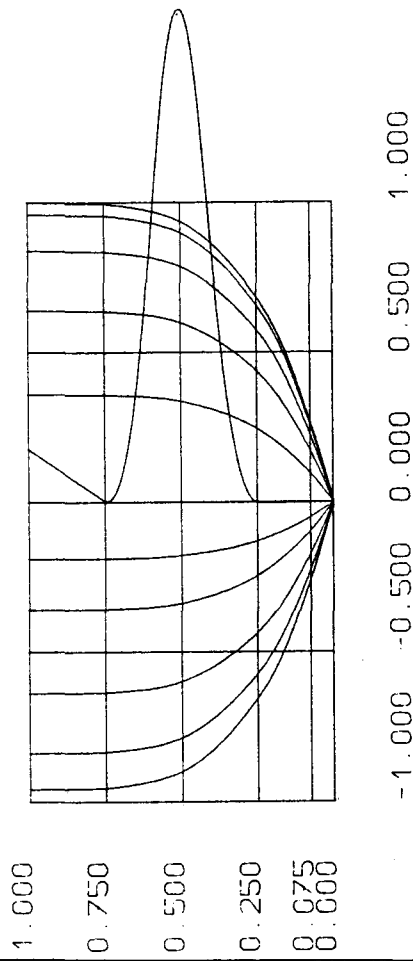
For the sake of comparison, the results of computation made by Hsiung were put in the same Fig. 8(b). From this two figures, it is clear that as $H \rightarrow \infty$ the results from Sretenski's formula agreed well with results from Michell's integral.

In order to recognize the influence of restricted water depth on the optimal ship forms, we optimized the same model under the same condition as in the previous cases and depth Froude number was taken as $F_h = 0.876$. The produced optimal forms, which were subject to the same constraints $y_{2j} \leq 0$ and $0 \leq y_{2j} \leq 1$, are shown in Figs. 10 and 11 respectively. In addition to that, y_{2j} was fixed at zero in the latter so that limited solution can be obtained. It is clear from the pictures that there is much more difference between the shallow-water and the deep-water optimal ship form for minimum wave resistance.

It would be more practical to select certain real ship form so as to produce optimal ship forms under appropriate restraints. For the sake of comparison with some results which have already appeared /1/, the Series 60, Block 60 was also chosen for developing the optimal ship forms in shallow water. The hull of Series 60, Block 60, before optimization, is shown in Fig. 12. In the optimization process, all given part of body was fixed at the Block 60 hull from Series 60. Also the design water-line area and tangent line (outline of the flat part of the bottom) were fixed at those of the Series 60 hull.

The following inequalities were imposed (see page 28):

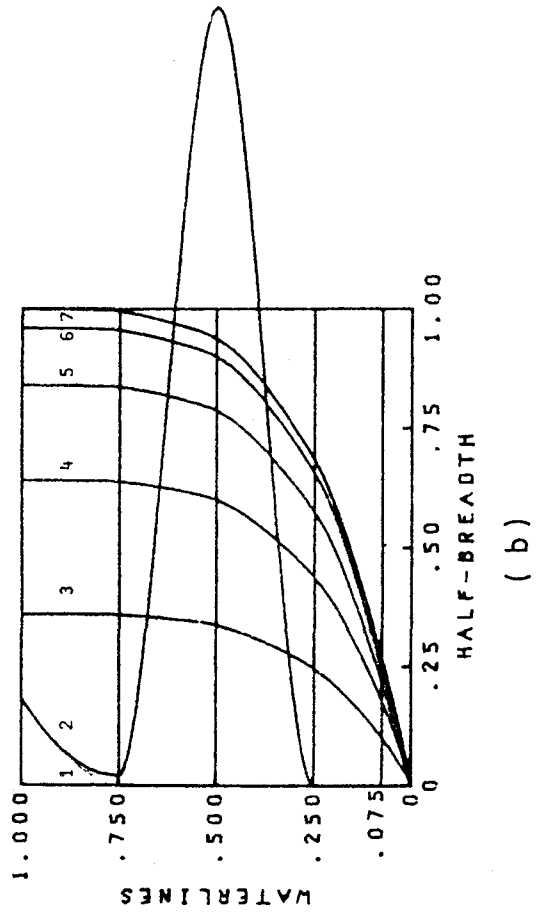
SECTION LINES



CR0=0.112
CR1=0.0986

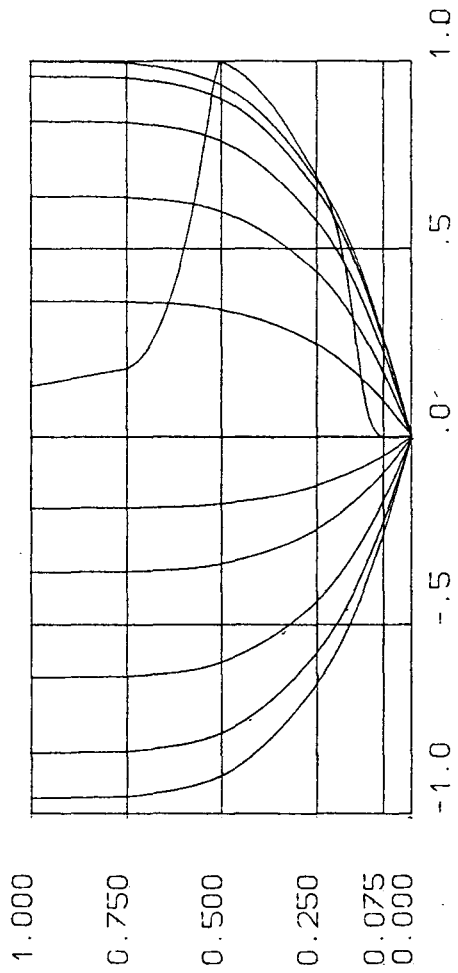
(a)

Given afterbody
 $y = (1-x^2)(1-z^4)$
 (origin midships and DWL)
 $T/L = .10, F_n = .316$
 $y_{2j} \geq 0$
 Original C_R of $y=(1-x^2)(1-z^4)$
 at $F_n = .316 : C_R = .112$
 Minimized $C_R : \tilde{C}_R = .0988$



(b)

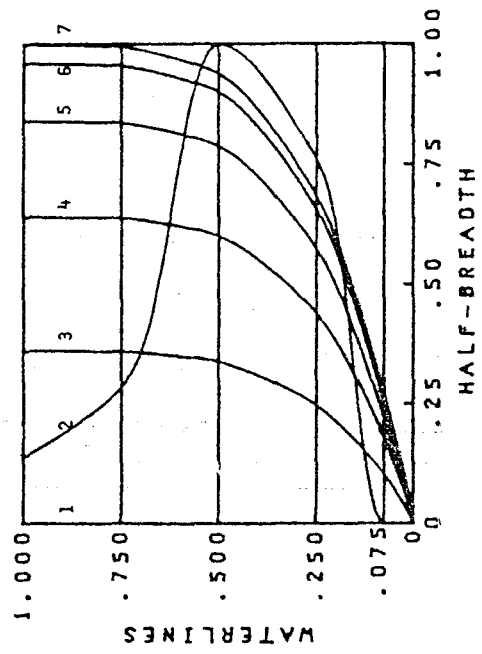
Fig. 8



HALF BREADTH

(a)

Given afterbody
 $y = (1-x^2)(1-z^4)$
 (origin midships and DWL)
 $T/L = .10, F_n = .316$
 $0 \leq y_{2j} \leq 1$
 $C_R = .112 ; \bar{C}_R = .0989$



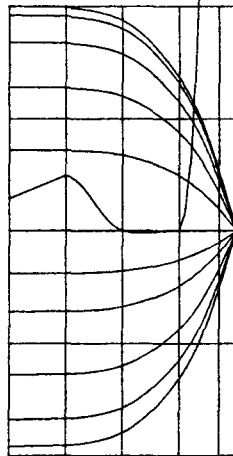
(b)

Figure 9

FN= 0.316
FH= 0.876
Q= 5.000
CR0=0.165
CR1=0.114

SECTION LINES

1.000
0.750
0.500
0.250
0.000

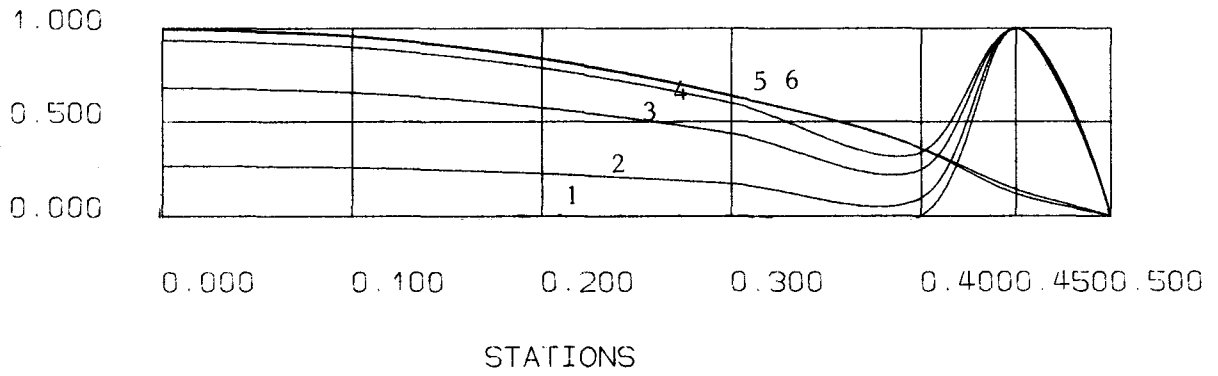


-1.000 -0.500 0.000 0.500 1.000

HALF BREADTH

Fig. 10

WATER LINES



FN= 0.316

FH= 0.876

Q= 6

CR0=0.165

CR1=0.116

SECTION LINES

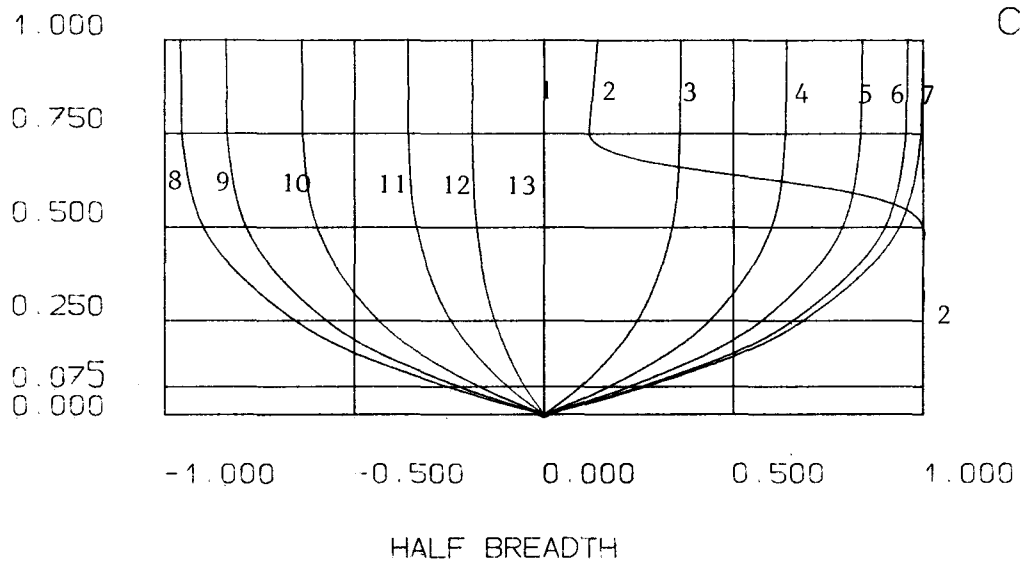
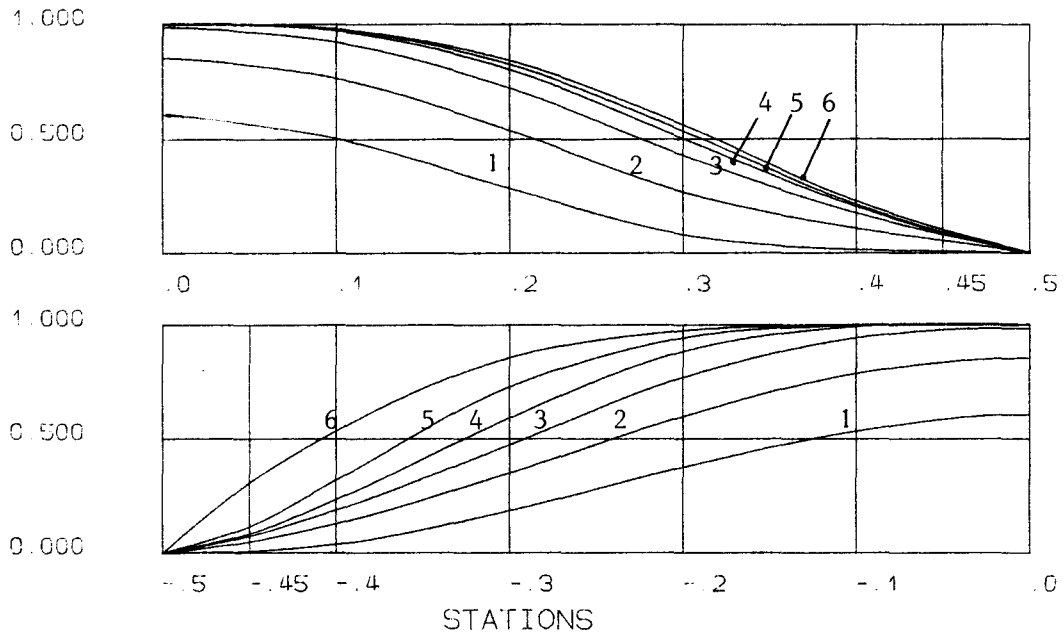


Fig. 11

WATER LINES



SECTION LINES

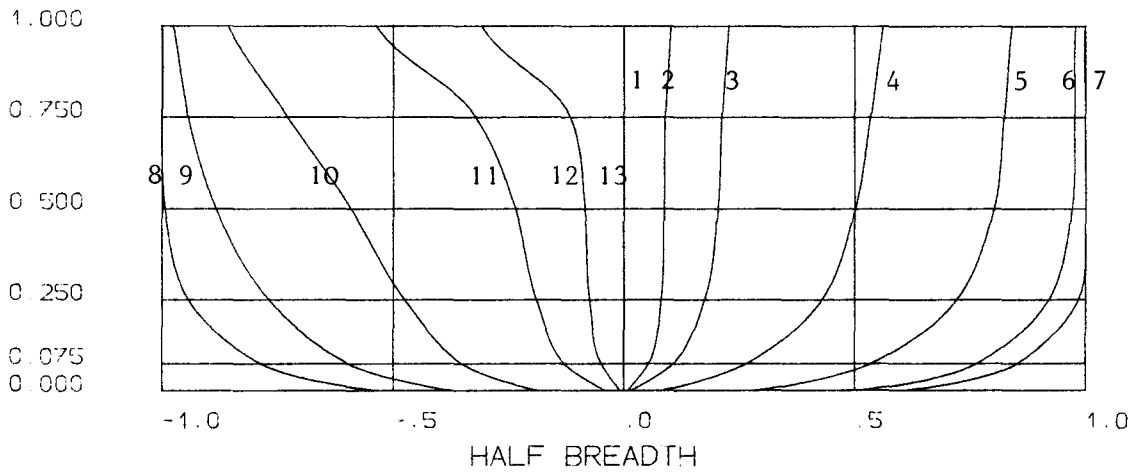


Fig. 12

1) One of the following constraints of unknown offsets:

L_R	constraints for unknown offsets
1	$A_o \leq Y_{ij} \leq B_o$
2	$A_o \cdot Y_{ij}^{(60)} \leq Y_{ij} \leq B_o \cdot Y_{ij}^{(60)}$
3	$A_o \leq Y_{ij} \leq B_o \cdot Y_{ij}^{(60)}$
4	$A_o \cdot Y_{ij}^{(60)} \leq Y_{ij} \leq B_o$

Here $Y_{ij}^{(60)}$ -- offsets of the Series 60, Block 60;

2) Section-angle constraint, i.e.,
the angle of section-line $\geq 10^\circ$ at Stations 2,3,4;

3) Water-plane-area constraint, i.e.,
 $C_{wp} = C_{wp}^{(60)}$;

4) Displacement constraint:

$$C_b^{(60)} \leq C_b \leq C_b^{(60)} + C_b \quad \text{for } C_b > 0$$

or

$$C_b^{(60)} + \Delta C_b \leq C_b \leq C_b^{(60)} \quad \text{for } C_b > 0$$

Here C_b -- allowed amount to change block coefficient.

The Results of Optimization for Total Resistance

First we computed optimal forms for a few cases of different constraints to see what feature an optimal ship form under the shallow water condition is. The results are shown in Figs. 13-20. The first four figures are for deep water and Froude number was 0.289. The last four figures are for shallow water and Froude number was kept the same as in the former, and depth Froude number F_h was 0.919.

Although we tried to display the optimal forms for both deep water and shallow water under the same conditions, it is shown from present computations that even if the solution to the deep water problem can be attained, it does not mean existence of a solution to the shallow water problem under the same constraints, the reverse is true. This is because the same set of constraints might not be compatible for both of the problems.

The appearance of this case just shows that depth of water has vital influence on the optimal ship forms. After comparing with deep-water optimal forms, we find that shallow-water optimal forms in these figures have a feature in common, that is, they have a well-distributed value of bulbous bow along the length of ship but even wilder in depthwise direction than that in deep water under the same conditions.

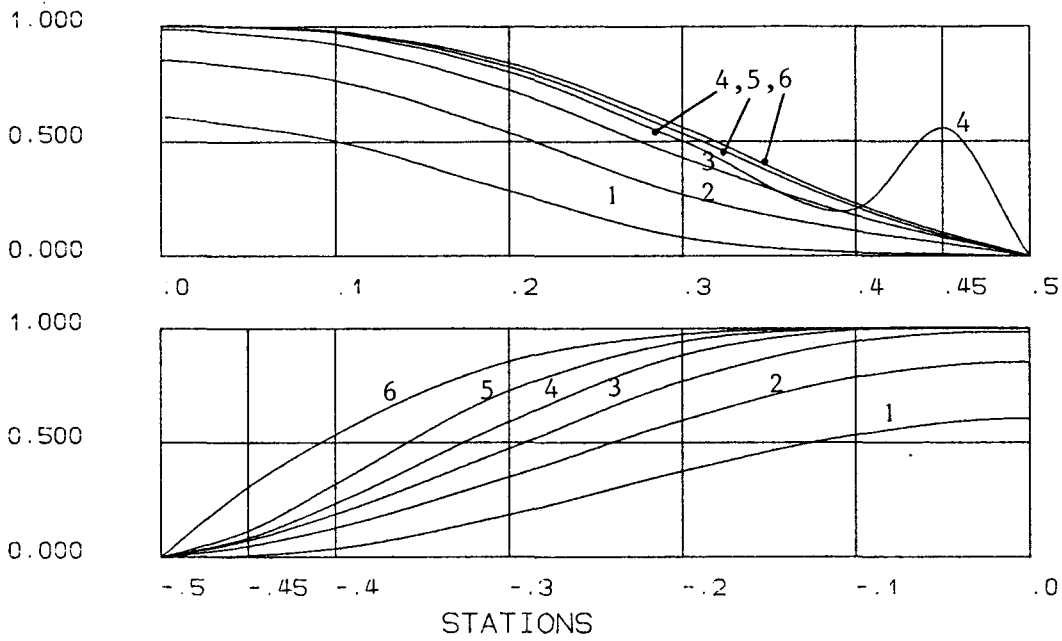
Figs. 21-24 show optimal ship forms for shallow water minimum total resistance (without taking form factor into account). It is shown from the present computations that there are some similar pictures to the case mentioned above i.e., although exactly under the same conditions to optimize ship forms for minimum wave resistance and for minimum total resistance, there is the possibility that the solutions of both cases do not exist simultaneously. Generally speaking, since the frictional resistance, which was taken as proportional to the hull surface area, was added to the object function of optimization problem, this device will not only function as a brake upon wild behavior of the optimal forms for wave resistance but also may influence the question if the solution exist or not. For

example, there is no existence of a solution to the optimization problem for minimum wave resistance, but there exist the solution to the optimization problem for minimum total resistance as shown in Fig. 25 and a opposite case is shown in fig. 26.

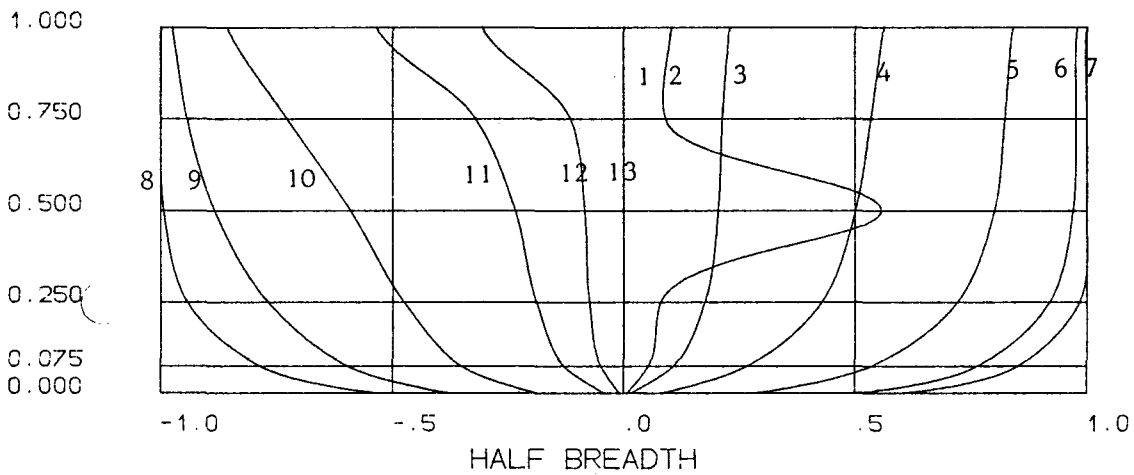
We may be able to produce some practical optimal ship forms if the unknown offsets are allowed to vary in only a narrow range and appropriate restrictions, which seem to be consistent with a sensible application, are imposed. The last three Figs. of 27 to 33 are for shallow water ($F_h = 0.919$ or 0.945). From these six pictures, we might say, as stated by Hsiung in his paper, "Because of the narrow-band constraint at the bow portion no bulb can possibly form there. However, it seems that the bulb is pushed back towards midship, forming some kind of wavy hull at the forebody of the ship". That is true for both deep water and shallow water.

Additionally, we find that there is a noticeable difference between the shallow water and the deep water optimal ship forms, i.e., the former always does not have such wild behavior as the latter along waterlines and always forms no midship bulb. This means that the shallow-water optimal ship forms generally require to have a larger prismatic coefficient.

WATER LINES



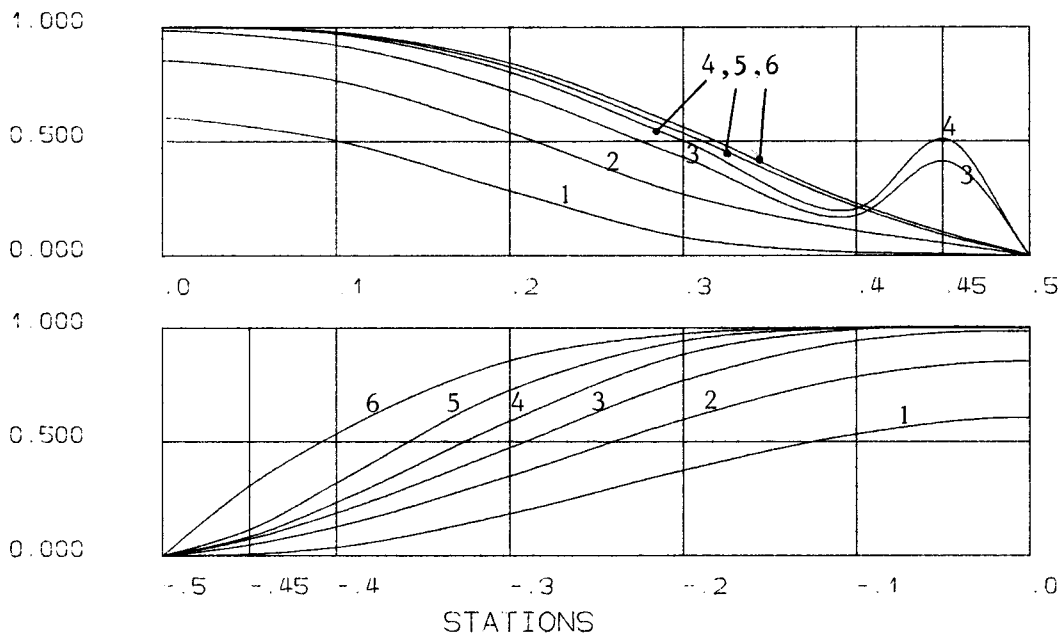
SECTION LINES



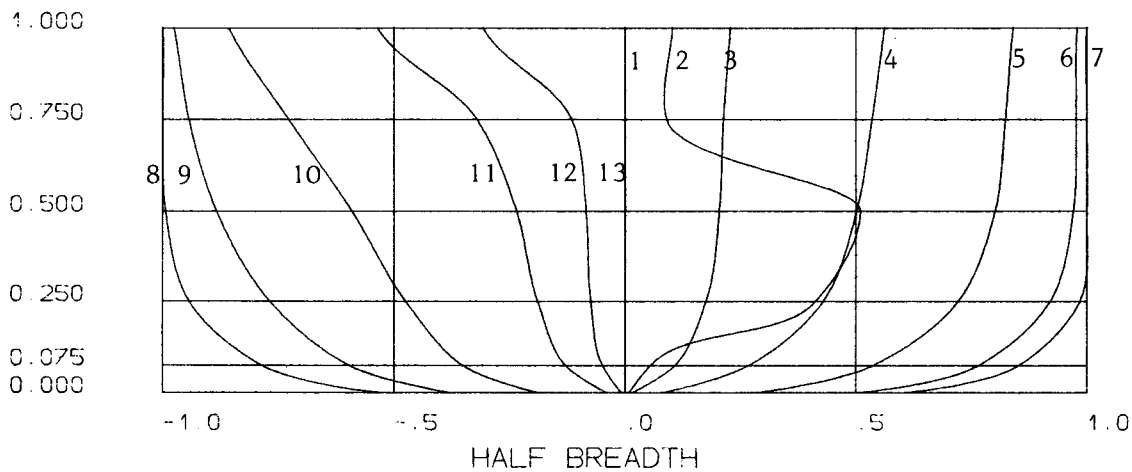
- FN- 0.289
- FH- 0.000
- Q- 25.
- CR0-0.204
- CR1-0.169
- VD- 0.010
- LR- 2
- A0- 1.000
- B0- 9.000

Figure 13

WATER LINES



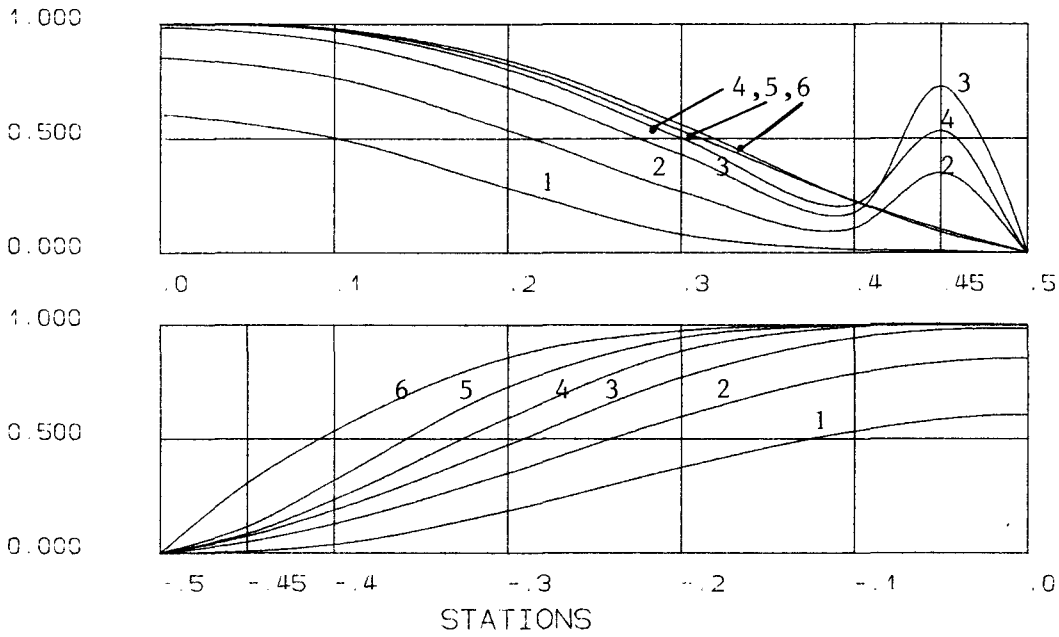
SECTION LINES



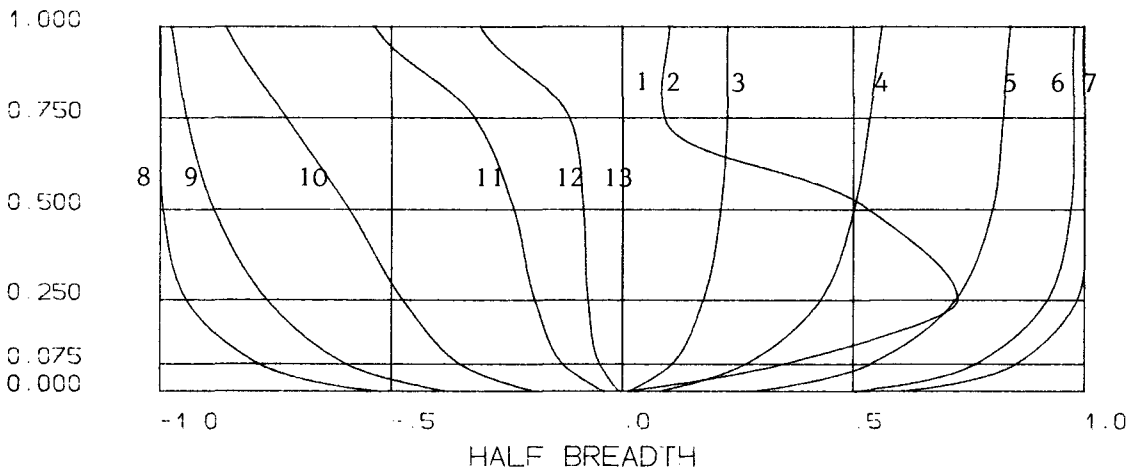
FN= 0.289
 FH= 0.000
 Q= 25
 CR0=0.204
 CR1=0.159
 VD= 0.015
 LR= 2.
 A0= 1.000
 B0= 9.000

Figure 14

WATER LINES



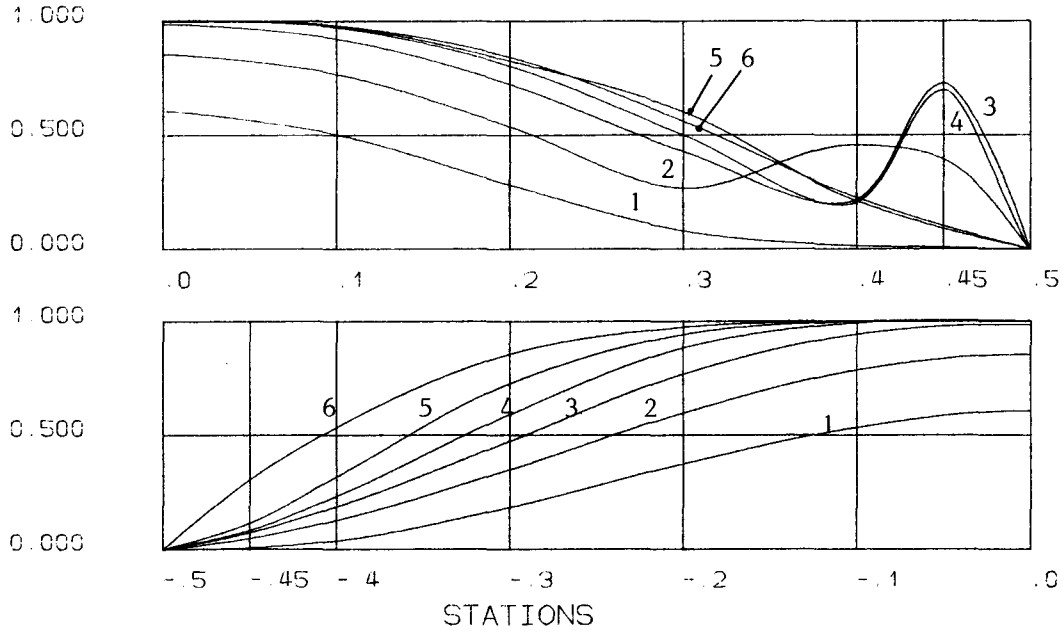
SECTION LINES



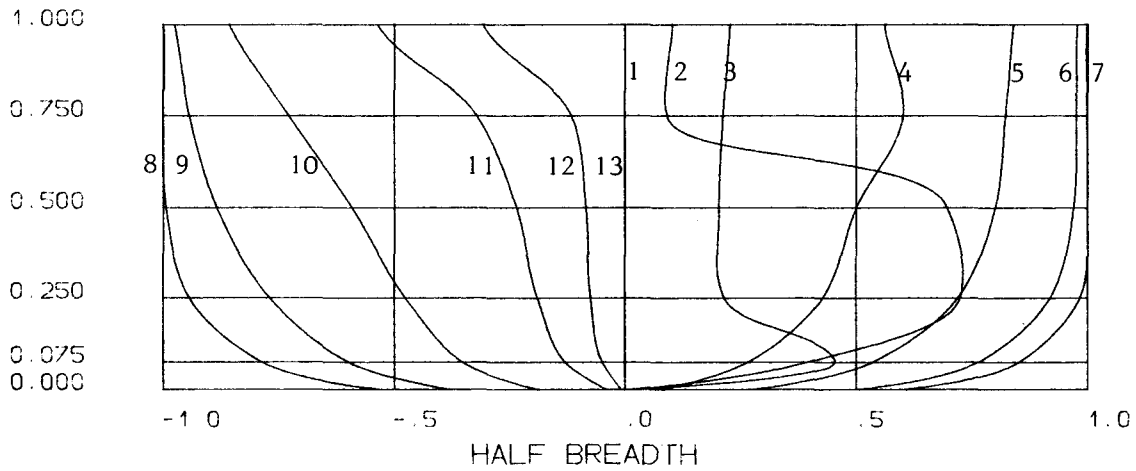
FN- 0.289
FH- 0.000
Q- 25
CR0-0.204
CR1-0.145
VD- 0.025
LR- 2.
A0- 1.000
B0- 9.000

Figure 15

WATER LINES



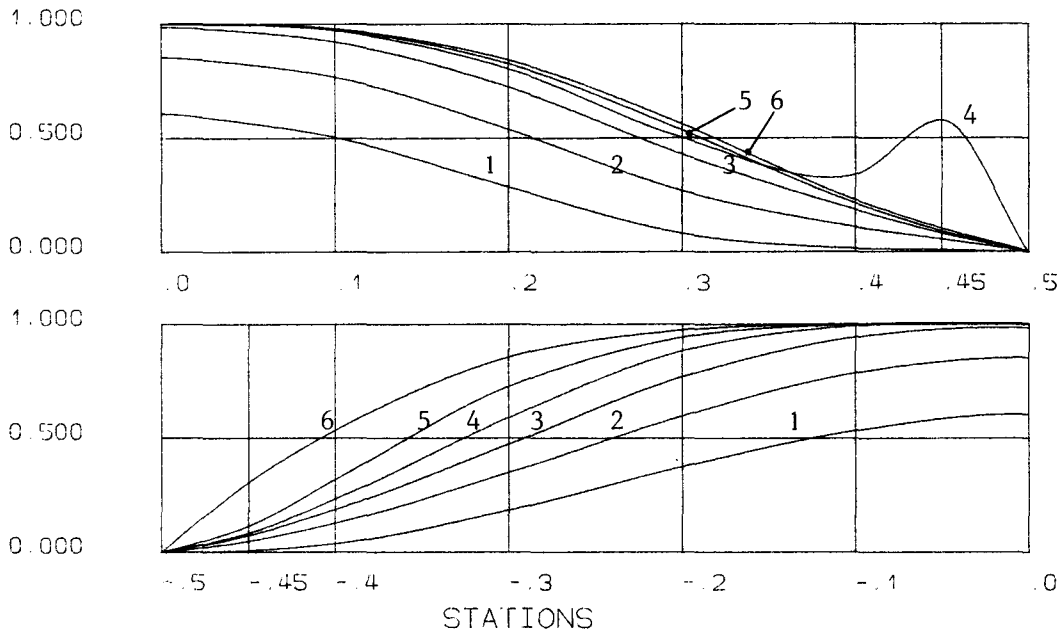
SECTION LINES



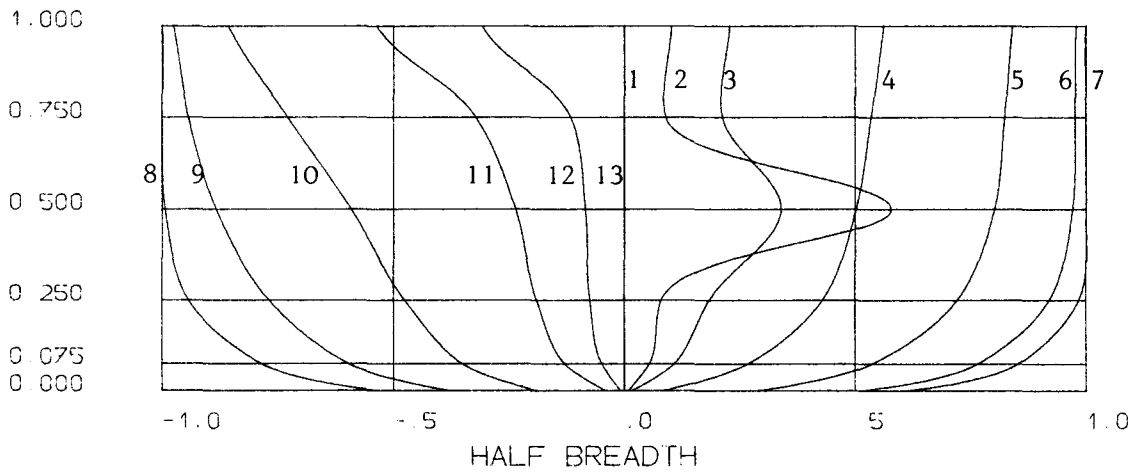
FN- 0.289
 FH- 0.000
 Q- 25.
 CR0-0.204
 CR1-0.141
 VD- 0.038
 LR- 2.
 A0- 1.000
 B0- 9.000

Figure 16

WATER LINES



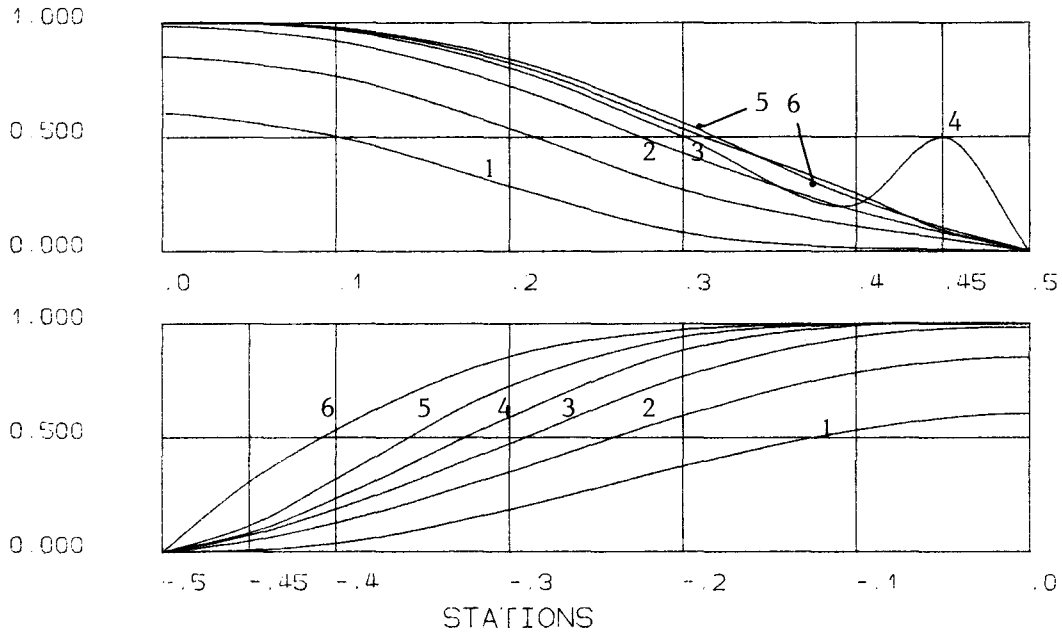
SECTION LINES



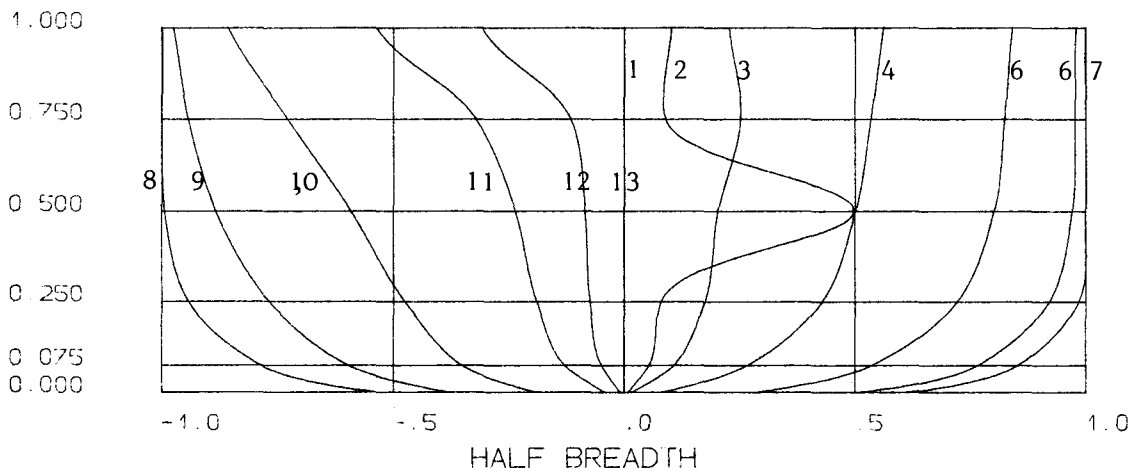
- FN- 0.289
- FH- 0.919
- Q- 25.
- CR0-0.517
- CR1-0.445
- VD- 0.015
- LR- 2.
- A0- 1.000
- B0- 9.000

Figure 18

WATER LINES



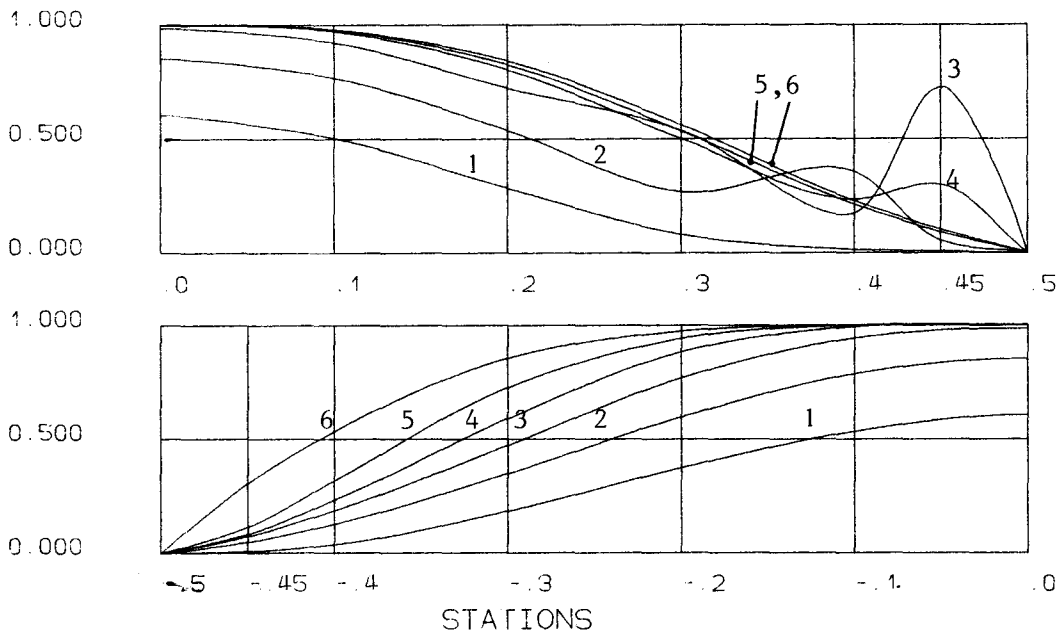
SECTION LINES



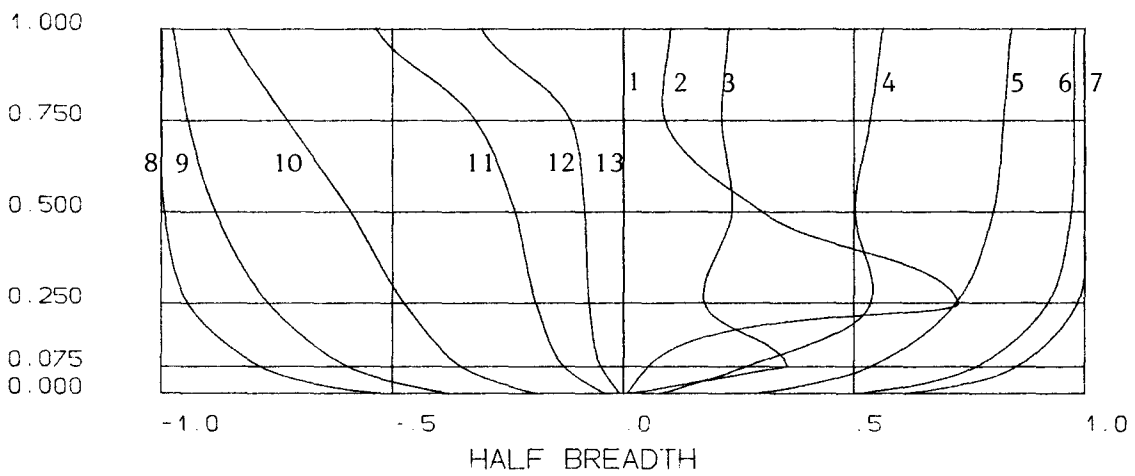
- FN- 0.289
- FH- 0.919
- Q- 25.
- CR0-0.517
- CR1-0.465
- VD- 0.010
- LR- 2.
- A0- 1.000
- B0- 9.000

Figure 17

WATER LINES



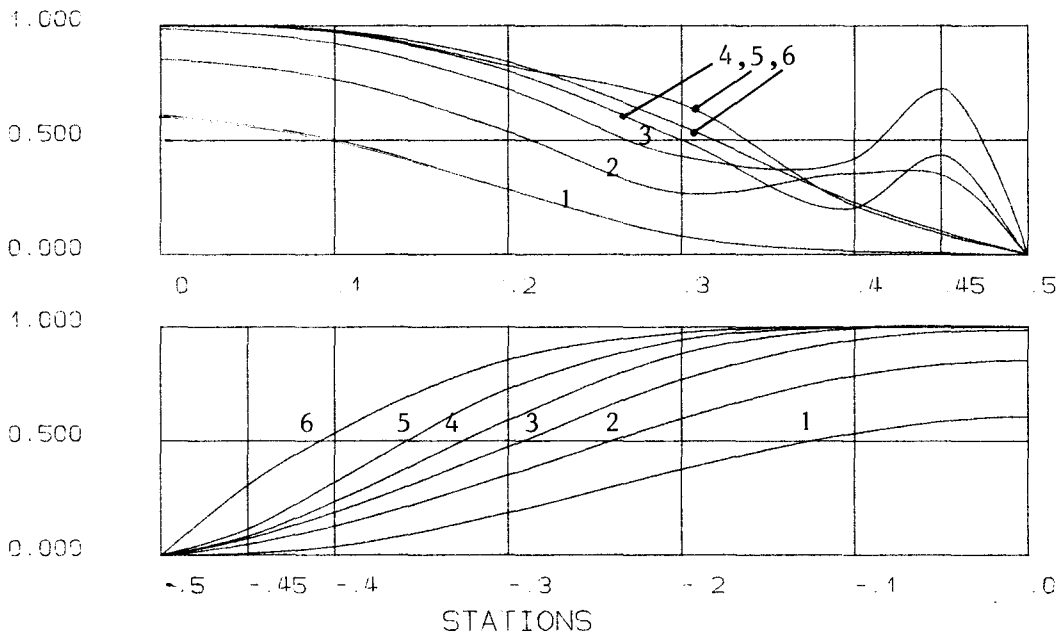
SECTION LINES



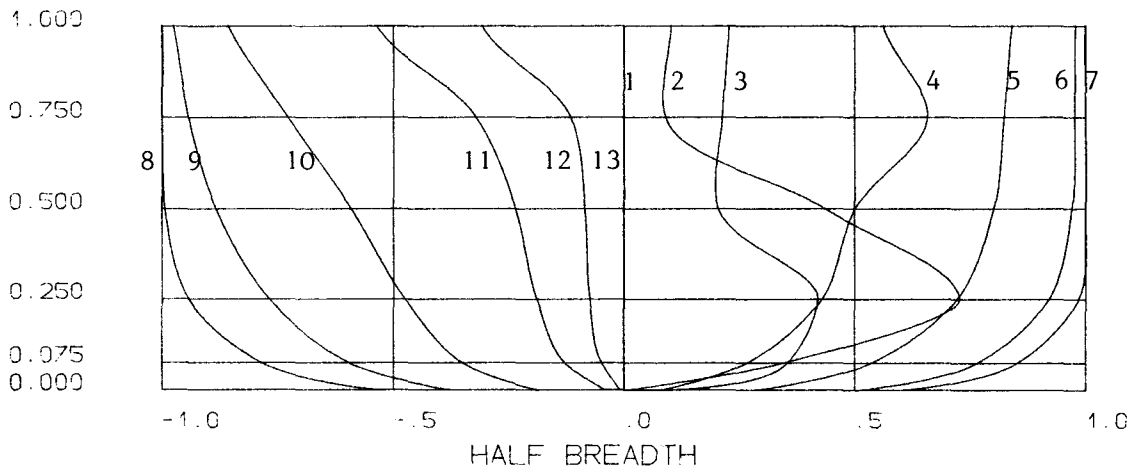
- FN- 0.289
- FH- 0.919
- Q- 25.
- CR0-0.517
- CR1-0.416
- VD- 0.025
- LR- 2.
- A0- 1.000
- B0- 9.000

Figure 19

WATER LINES



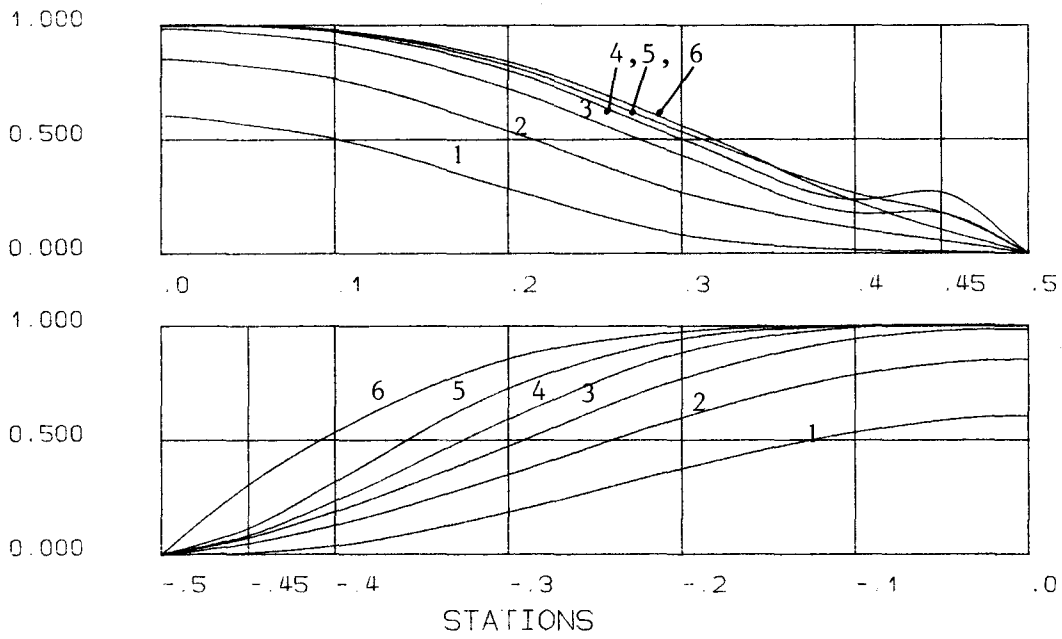
SECTION LINES



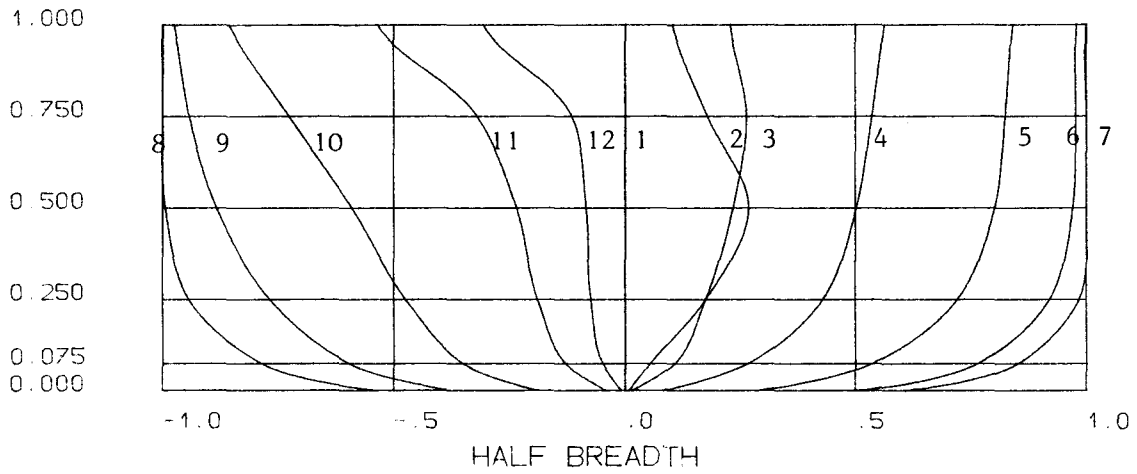
FN- 0.289
 FH- 0.919
 Q- 25.
 CR0-0.517
 CR1-0.380
 VD- 0.038
 LR- 2.
 A0- 1.000
 B0- 9.000

Figure 20

WATER LINES



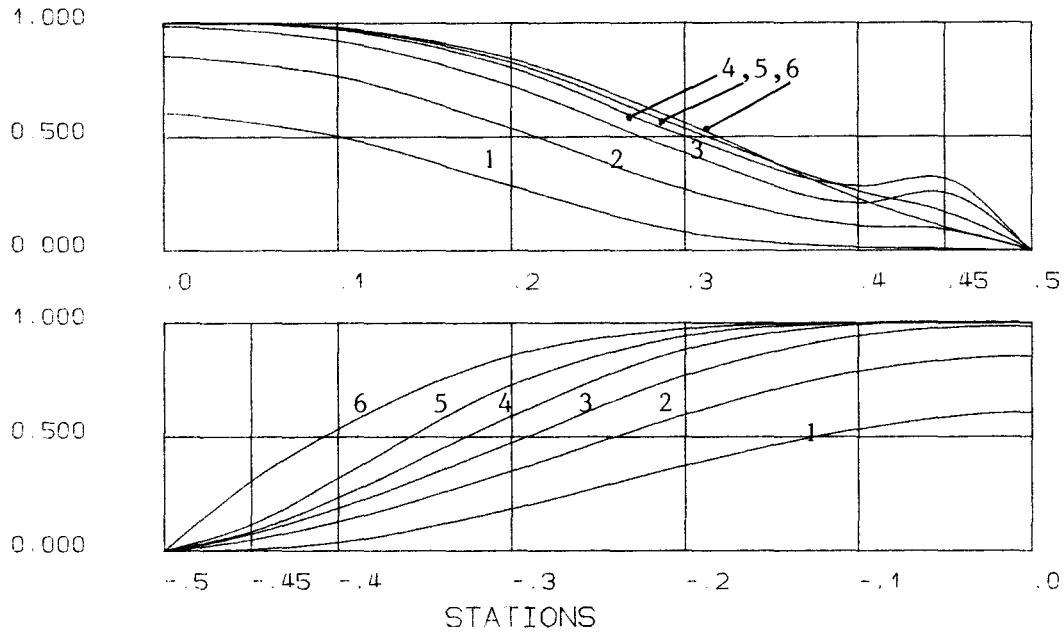
SECTION LINES



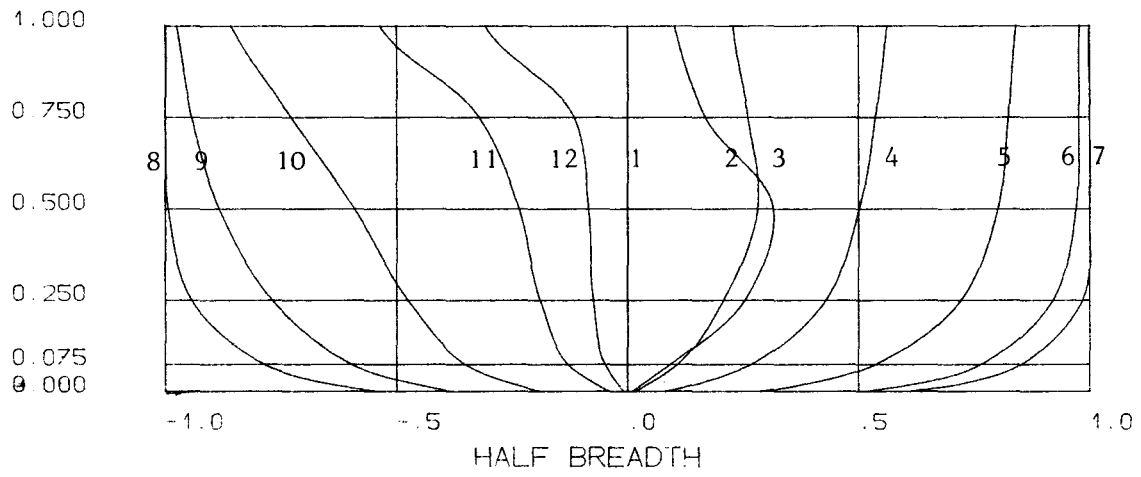
FN- 0.289 FH-0.919 Q- 25.
CT0 -0.751 CT-0.700 DELTA-0.010
LR -2. A0-1.000 B0-9.000

Figure 21

WATER LINES



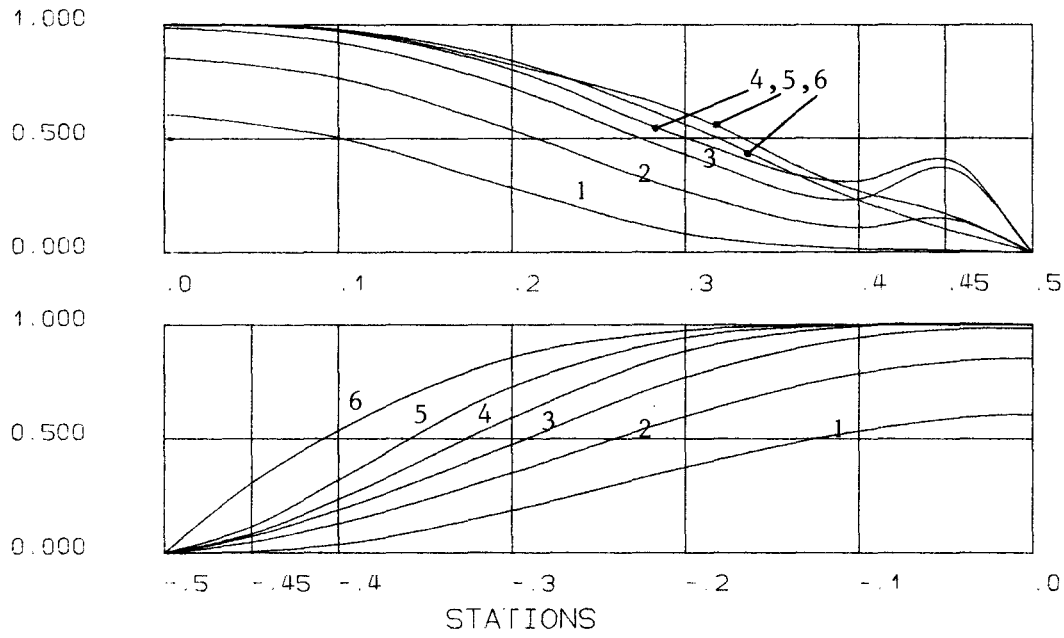
SECTION LINES



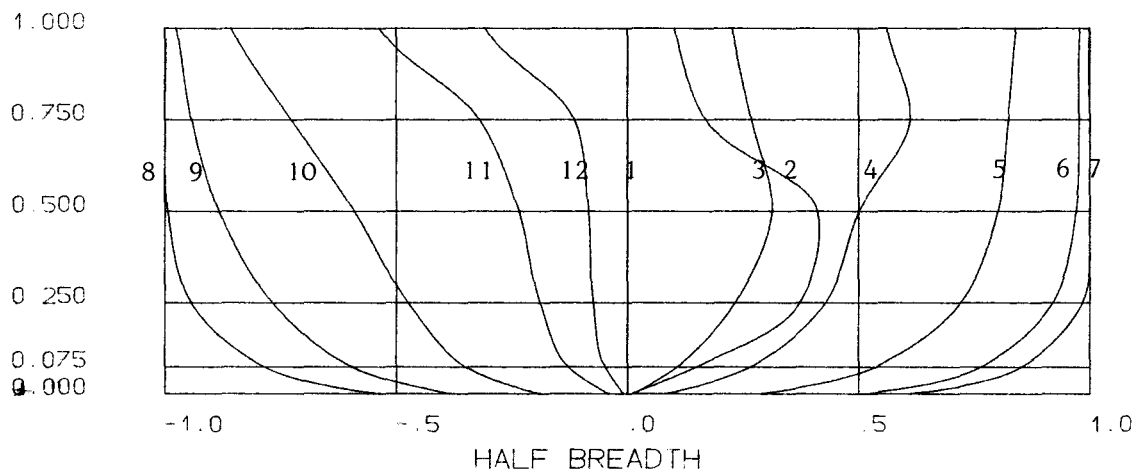
FN= 0.289 FH=0.919 Q= 25.
CT0 =-0.751 CT=0.682 DELTA=0.015
LR =-2. AC=1.000 BO=9.000

Figure 22

WATER LINES



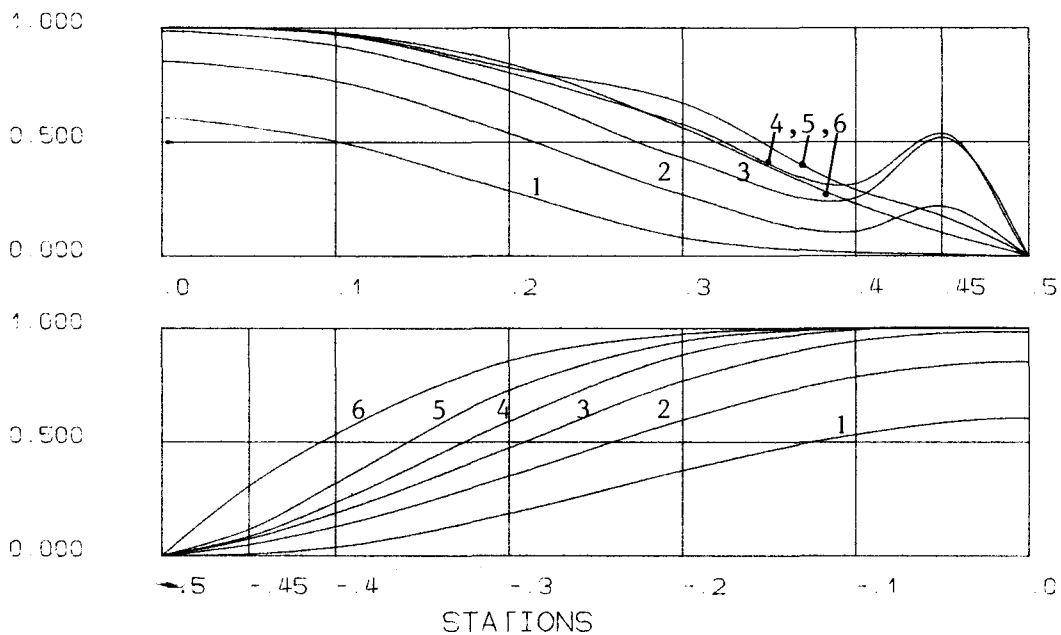
SECTION LINES



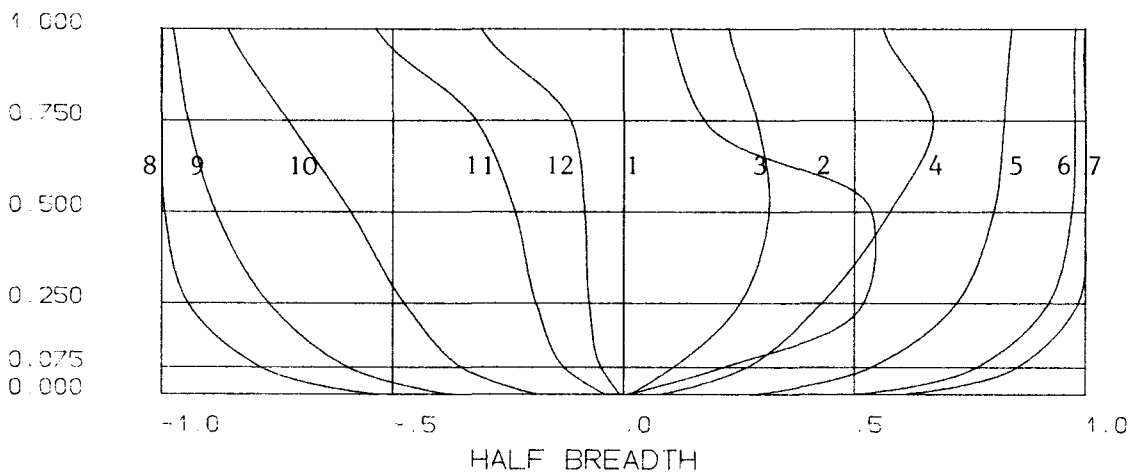
FN= 0.289 FH=0.919 Q= 25.
CT0 =0.751 CT=0.654 DELTA=0.025
LR =2. A0=1.000 B0=9.000

Figure 23

WATER LINES



SECTION LINES



FN- 0.289 FH-0.919 Q- 25.

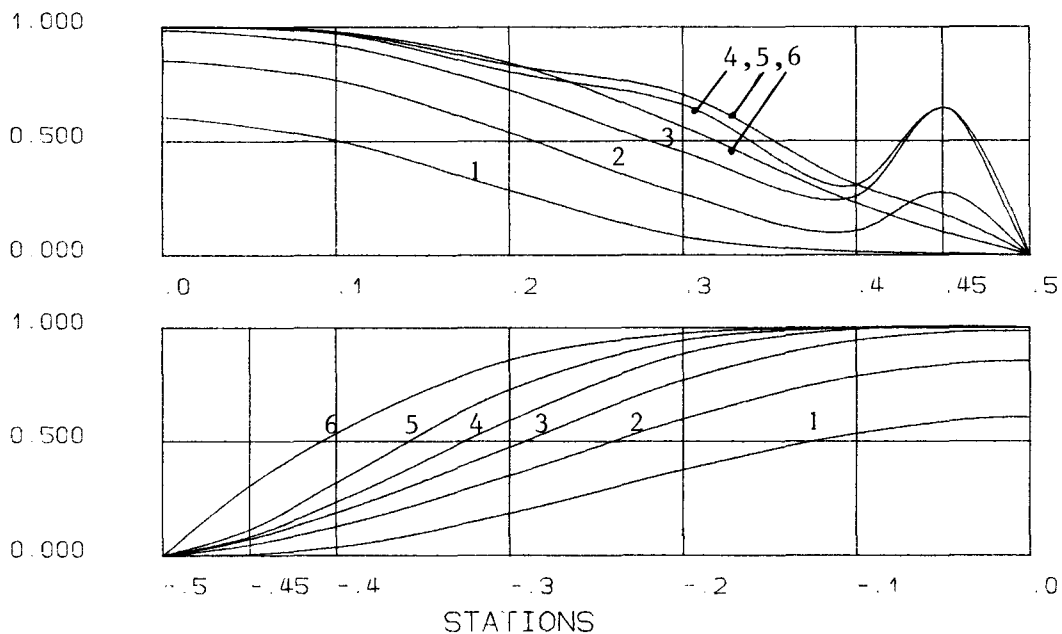
CT0 -0.751 CT-0.629 DELTA-0.038

CF0 -0.233 CF-0.244

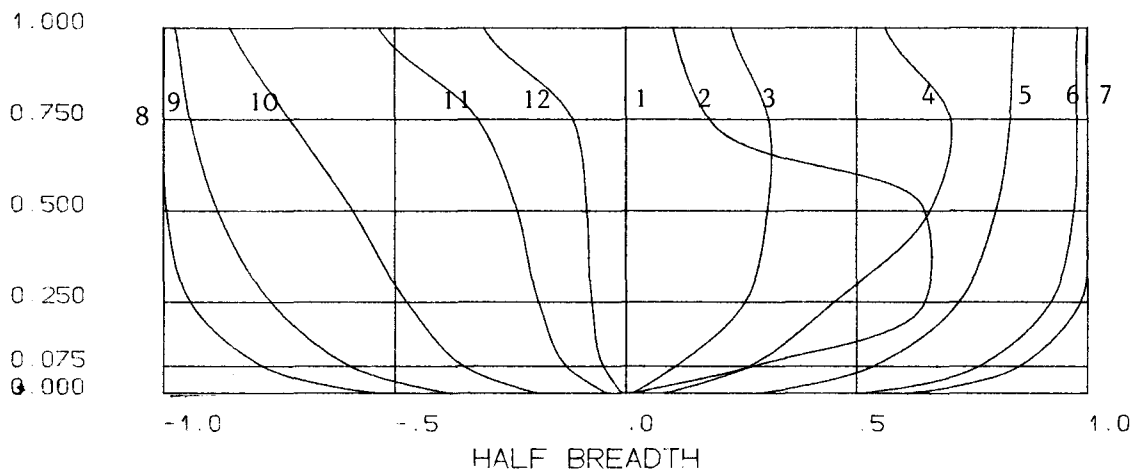
LR -2. A0-1.000 B0-9.000

Figure 24

WATER LINES



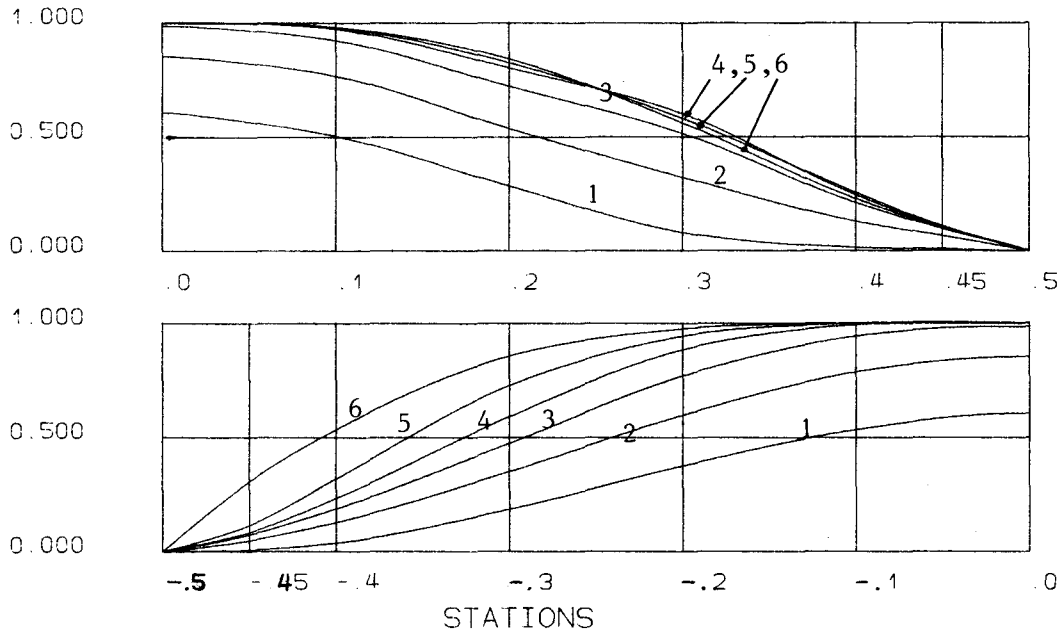
SECTION LINES



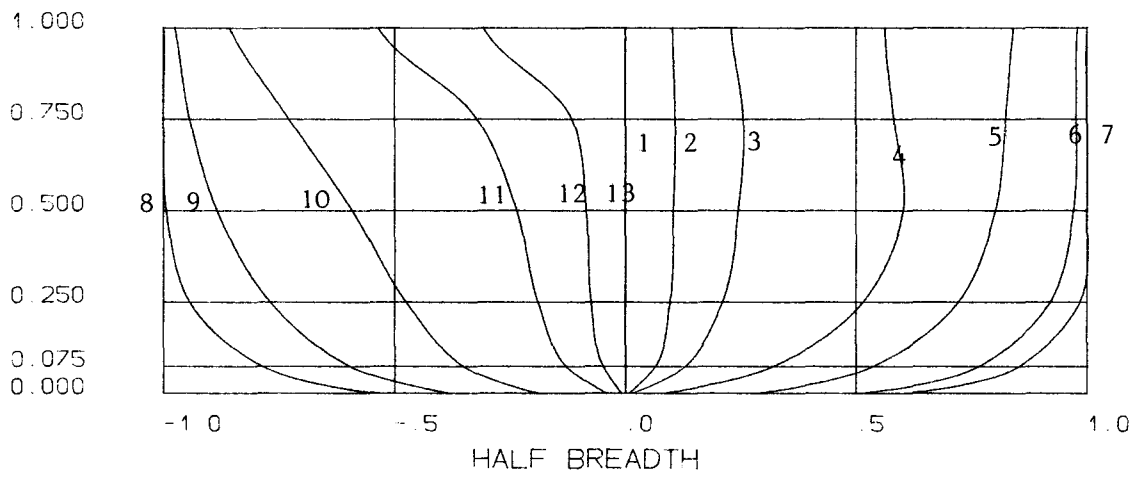
FN= 0.289 FH=0.919 Q= 25.
 CT0 =0.751 CT=0.616 DELTA=0.050
 LR =2. A0=1.000 B0=9.000

Figure 25

WATER LINES



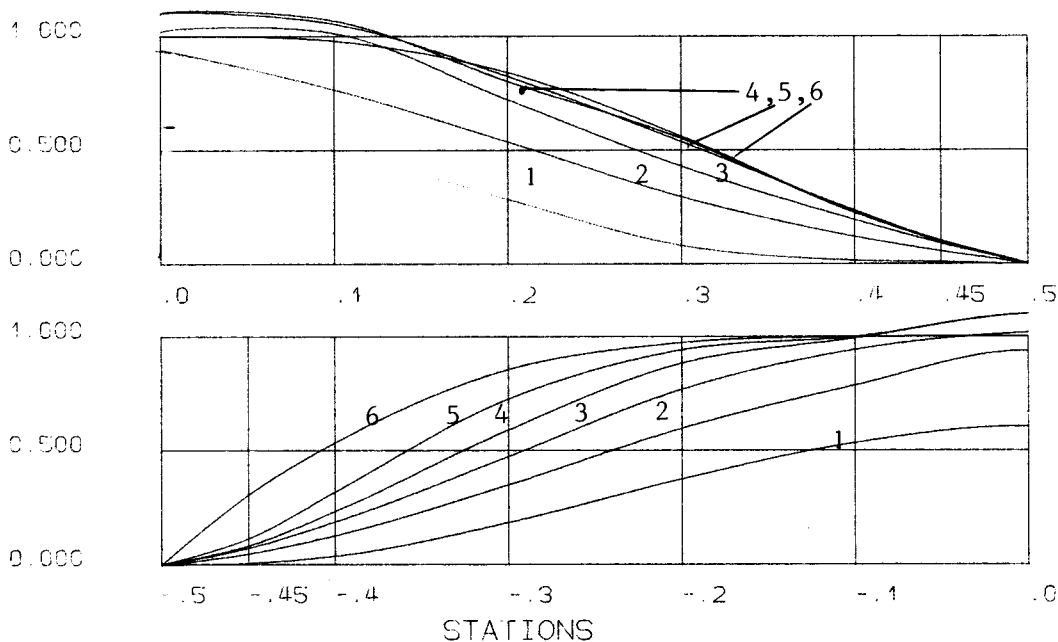
SECTION LINES



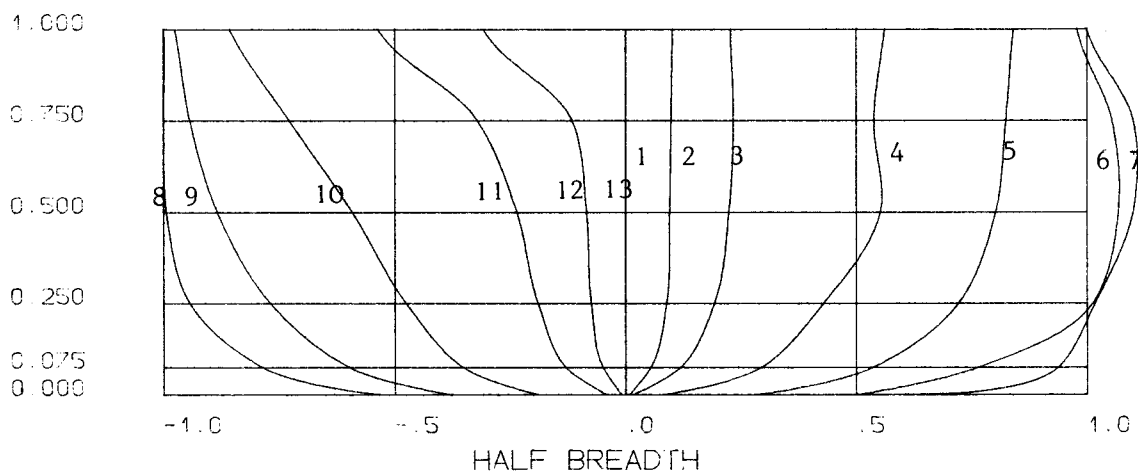
FN- 0.289
 FH- 0.919
 Q- 30.
 CR0-0.517
 CR1-0.478
 VD- 0.016
 LR- 2.
 A0- 1.000
 B0- 1.200

Figure 26

WATER LINES



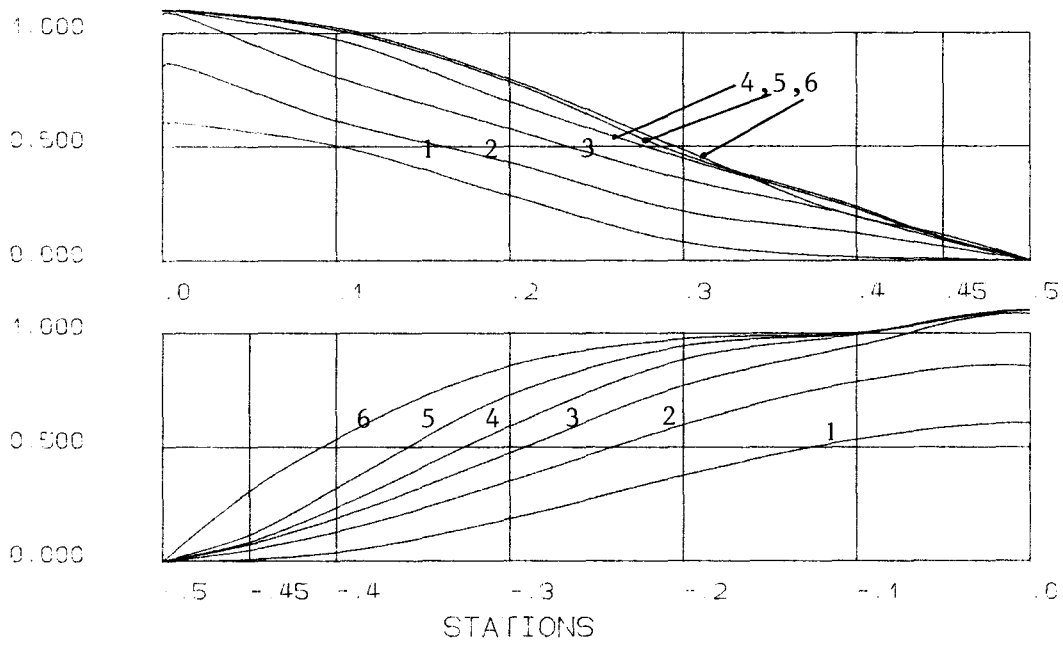
SECTION LINES



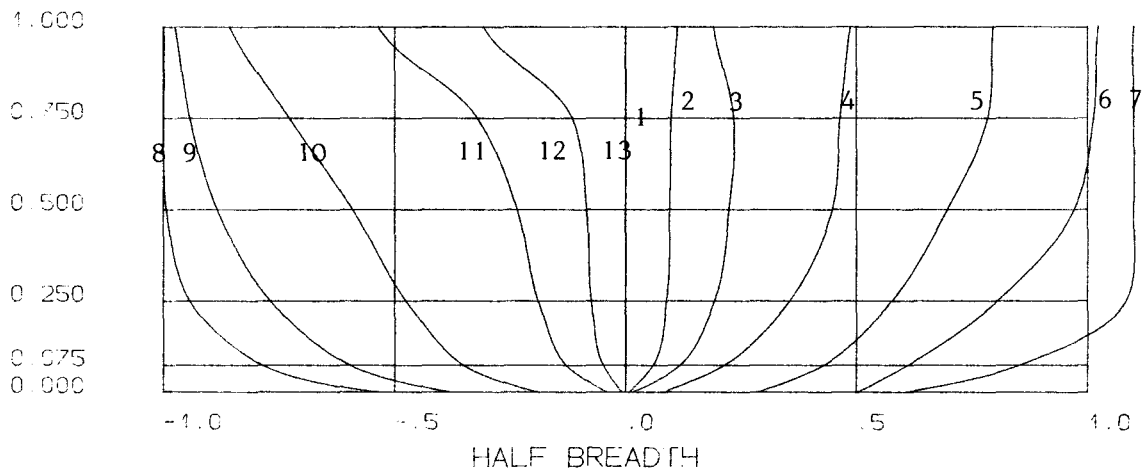
FN= 0.289 FH=0.000 Q= 30.
 CT0 =0.438 CT=0.418 DELTA=0.028
 LR =2. A0=1.000 B0=1.100

Figure 27

WATER LINES



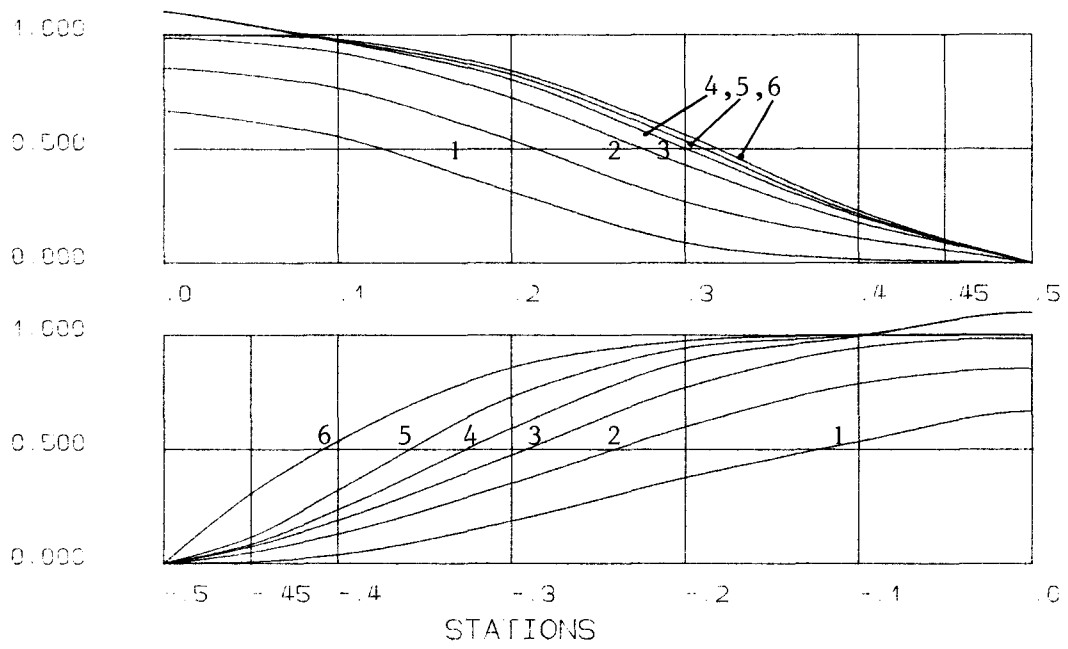
SECTION LINES



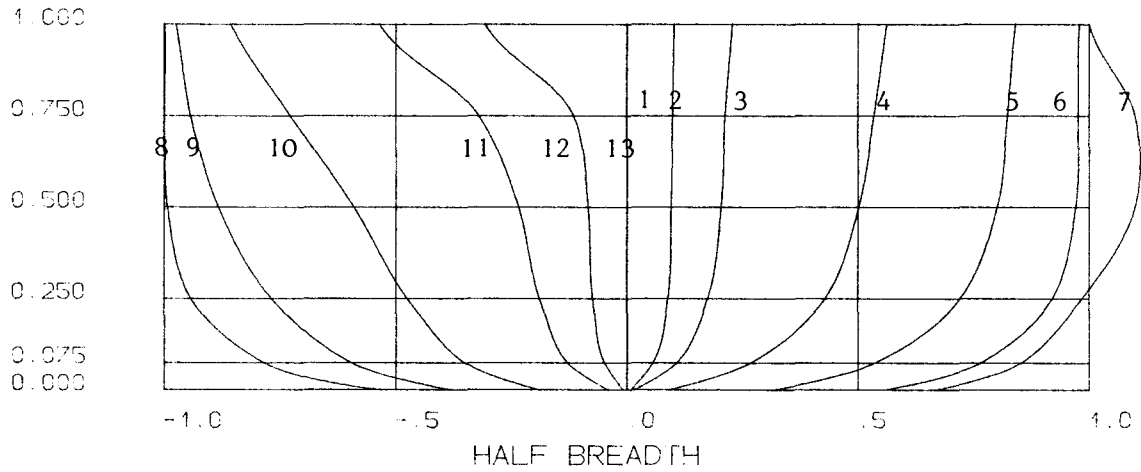
FN- 0.289 FH-0.0 Q- 30
CT0 -0.438 CT-0.333 DELTA--0.014
CF0 -0.233 CF-0.219
LR -2. A0-0.800 B0-1.100

Figure 28

WATER LINES



SECTION LINES



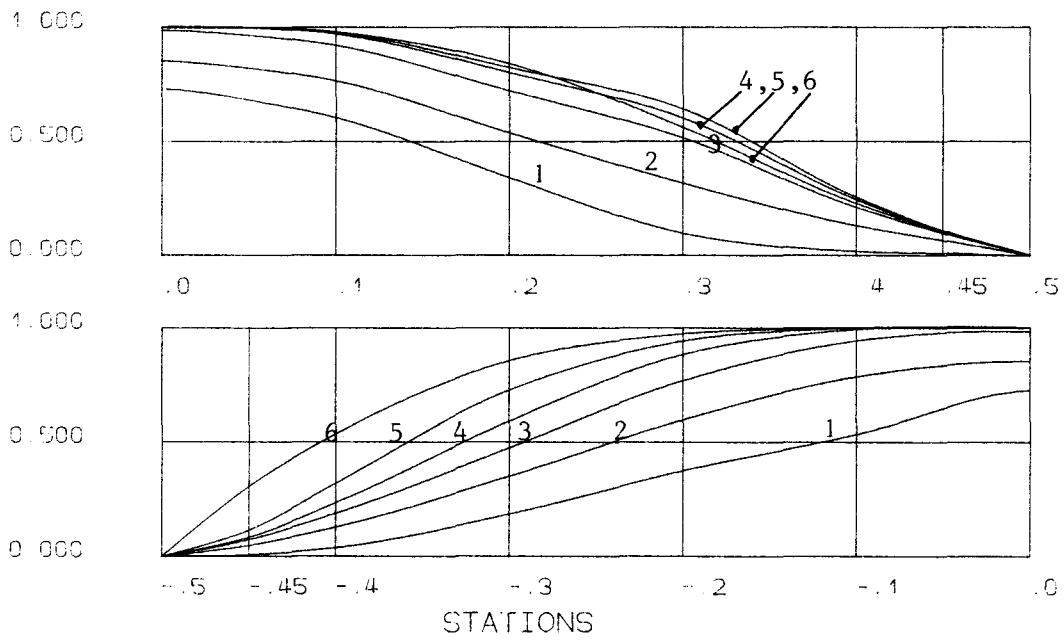
FN= 0.289 FH=0.000 Q= 36.

CTC =0.438 CT=0.394 DELTA=0.010

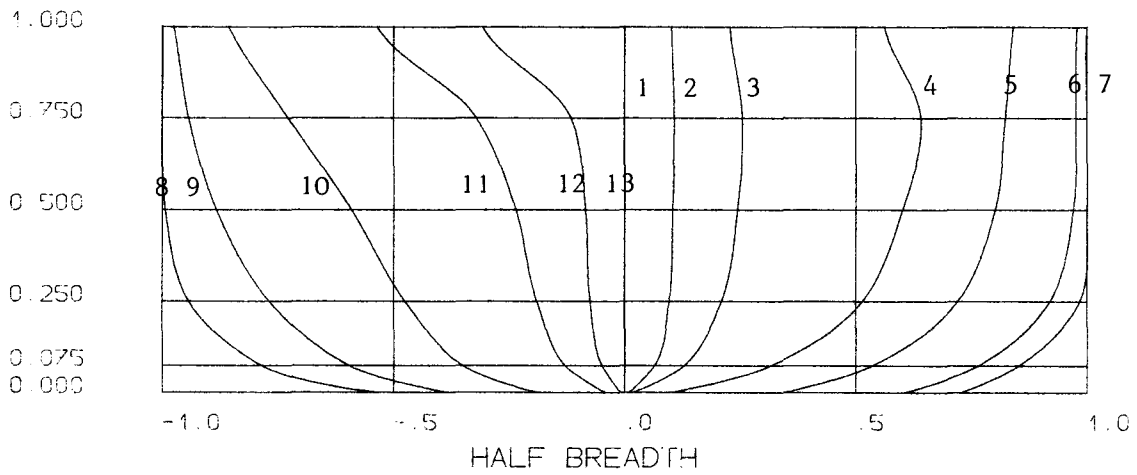
CF0 =0.233 CF=0.224

LR =2 AO=1.000 BO=1.100 **Figure 29**

WATER LINES



SECTION LINES



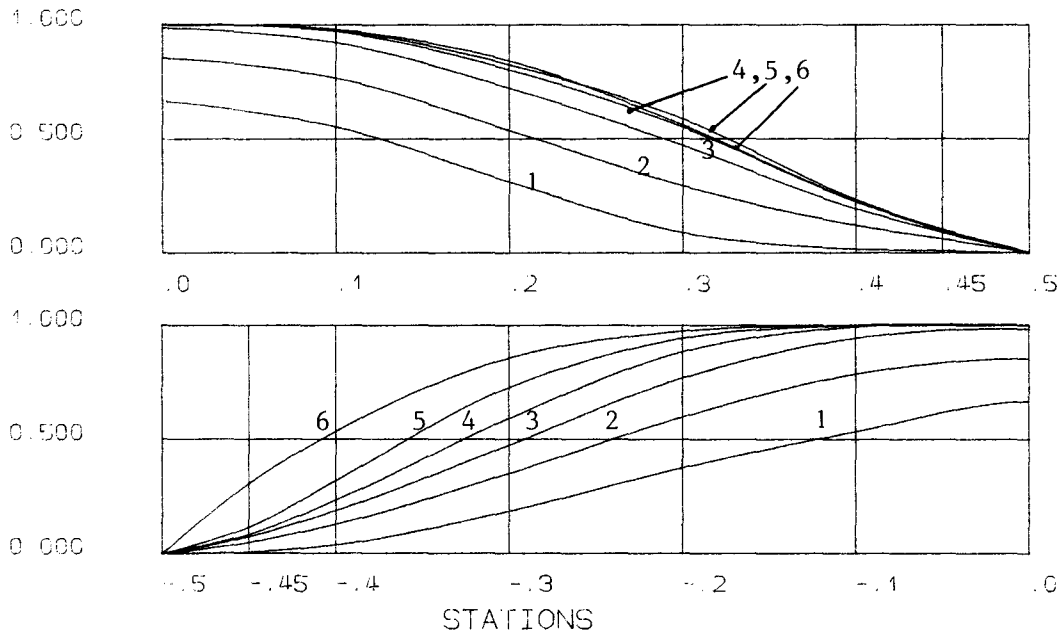
FN= 0.289 FH=0.945 Q= 36

CT0 =1.524 CT=1.437 DELTA=0.020

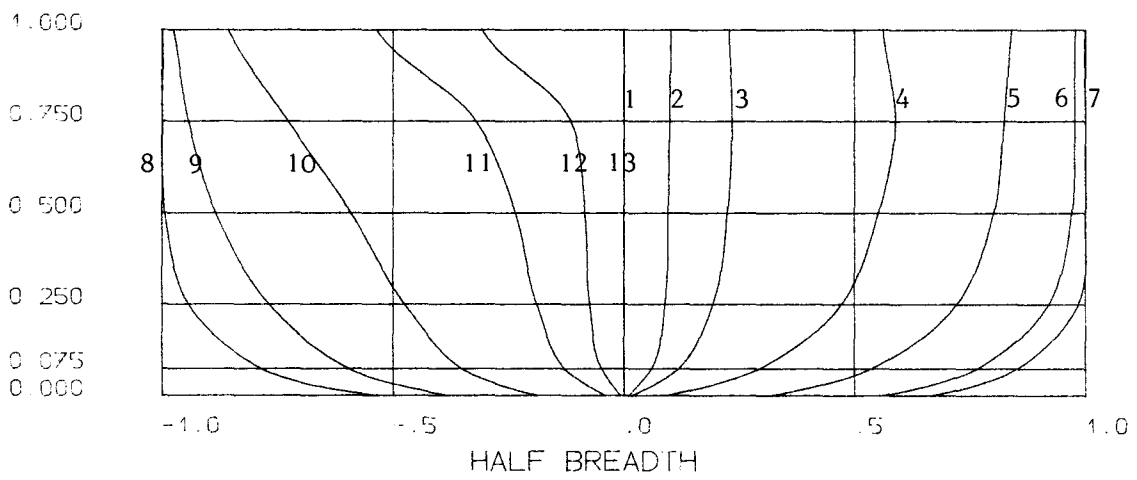
LR =2. A0=1.000 B0=1.200

Figure 30

WATER LINES



SECTION LINES



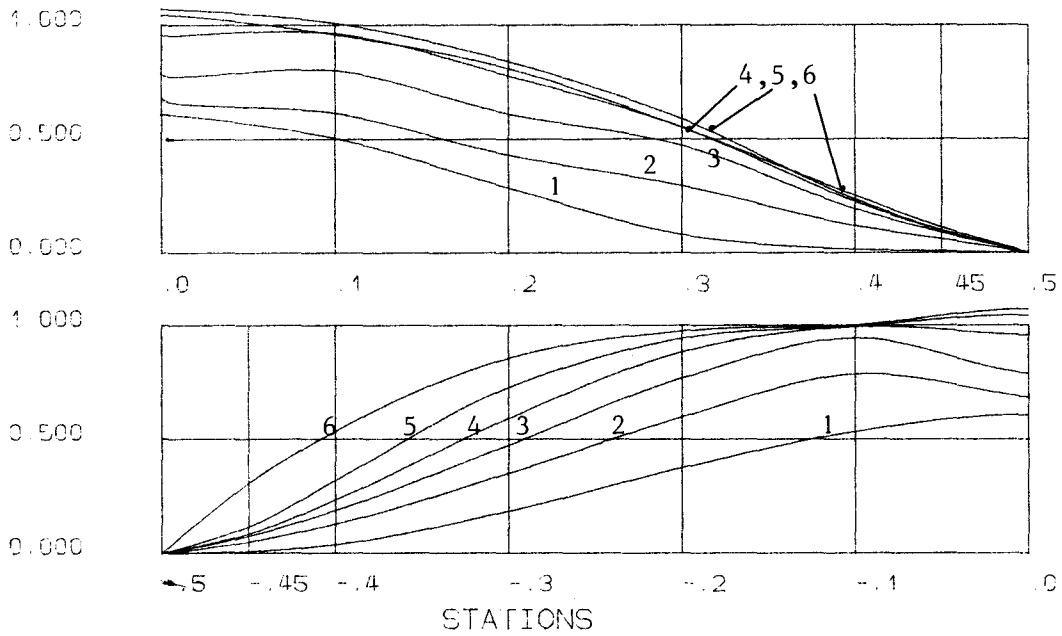
FN= 0.289 FH=0.945 Q= 36.

CTG =-1.524 CT=1.475 DELTA=0.010

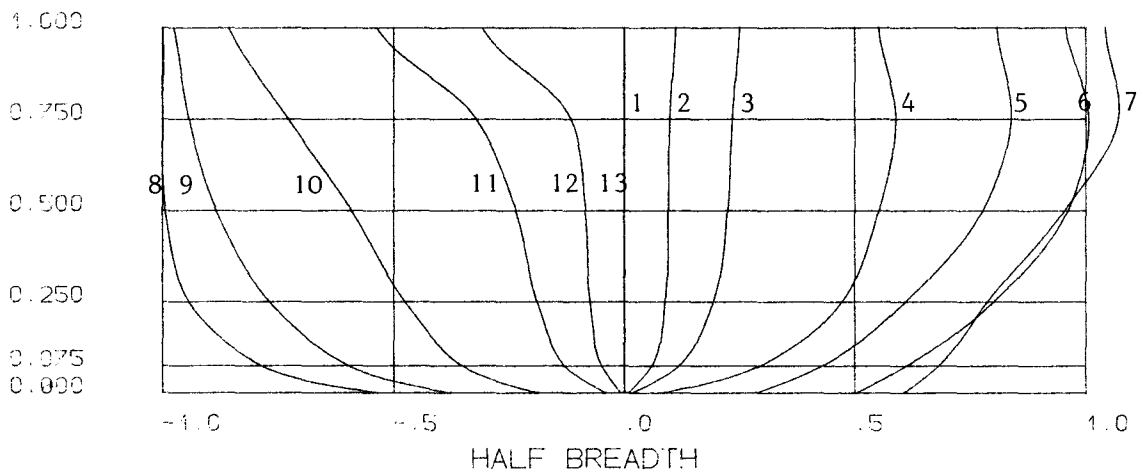
LR =-2. A0=1.000 B0=1.100

Fig. 31

WATER LINES



SECTION LINES



FN= 0.289 FH=0.919 Q= 30.

CTO =-0.751 CT=0.682 DELTA=-0.014

CF0 =-0.233 CF=0.215

LR =-2.0 A0=0.800 B0=1.100

Fig. 32

In other words, we might say that under the narrow-band constraint the ship displacement should be more distributed somewhat evenly towards the bow for the shallow-water optimal ship form (forming some kind of wavy hull) and on the other hand, the displacement should be concentrated towards the midship for deep-water optimal ship forms (forming some kind of side bulb).

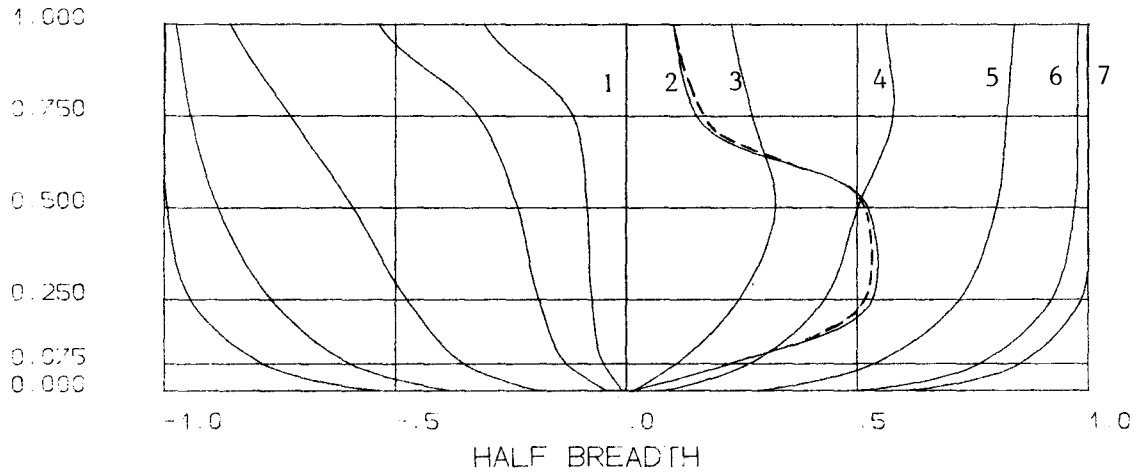
When the unknown offsets are allowed to vary in a large range, both of them form a bowbulb as shown in Fig. 33. But in addition to the bowbulb, deep-water optimal ship forms simultaneously form a side bulb, see Fig. 33(b).

Table 1 and 2 are respectively the offsets of solid lines and do not lines which was included the effect of form factor in Fig. 33(a). From here we may say that the effect of form factor is not great on the optimal ship form.

We also obtain some optimal afterbodies as shown in Figs. 34 and 35. Fig. 34 shows the optimal afterbody for deep water and Fig. 35 for shallow water. From the two pictures, we can also see the behavior of shallow-water optimal ship forms.

It is of interest to note that if we increase artificially the damping function of the viscous resistance, we can obtain close conventional ship forms which are willingly accepted by ship designer. Letting F to be the damping factor and replacing C_f by $F \cdot C_f$ in the objective function (23), we can reach the goal. Figs. 36(a), (b) and (c) show the optimal ship forms with given factors $F = 1, 100$ and 150 respectively and equal increment of 2 % displacement. From this feature, one perhaps expects it to be used in the Computer Aided Hull Form Design.

SECTION LINES

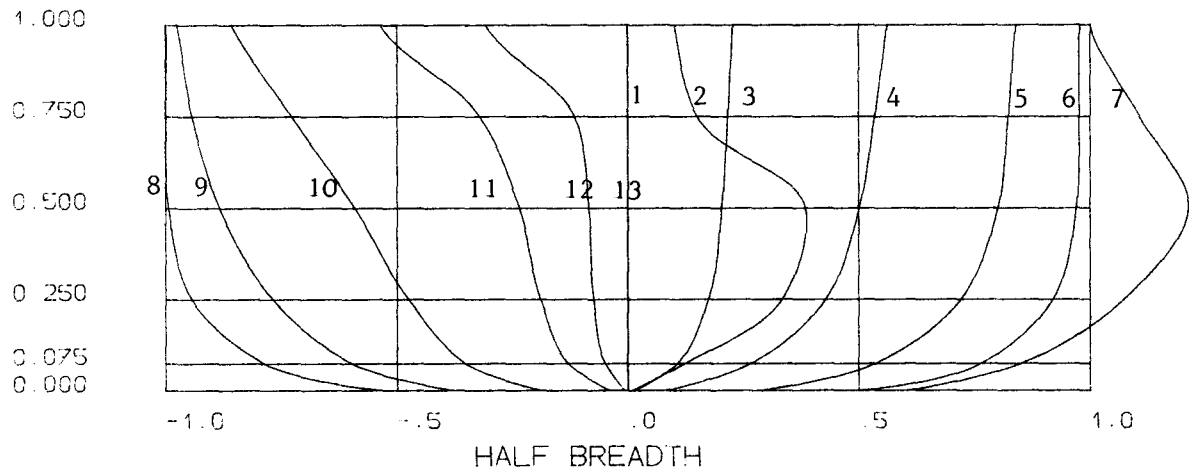


FN= 0.289 FH=0.945 Q= 30
CTC =-1.524 CT=-1.305 DELTA=0.030
CF0 =-0.233 CF=-0.243
LR =-2. A0=1.000 B0=9.000

— without form factor
----- with form factor

(a)

SECTION LINES



FN= 0.289 FH=0.000 Q= 30
CTC =-0.438 CT=-0.362 DELTA=0.030
LR =-2 A0=1.000 B0=9.000

(b)

Fig. 33

Table 1 Forebody offsets

j \ i	1	2	3	4	5	6	7
1	0.000	0.008	0.015	0.081	0.284	0.503	0.606
2	0.000	0.226	0.108	0.268	0.537	0.766	0.853
3	0.000	0.533	0.244	0.430	0.722	0.921	0.985
4	0.000	0.523	0.324	0.502	0.802	0.971	1.000
5	0.000	0.153	0.273	0.577	0.824	0.977	1.000
6	0.000	0.102	0.228	0.562	0.841	0.979	1.000

$F_n = 0.289, F_h = 0.945, q = 30$

$C_{to} = 1.524, C_t = 1.305, C_{fo} = 0.233, C_f = 0.243$ (without form factor correction)

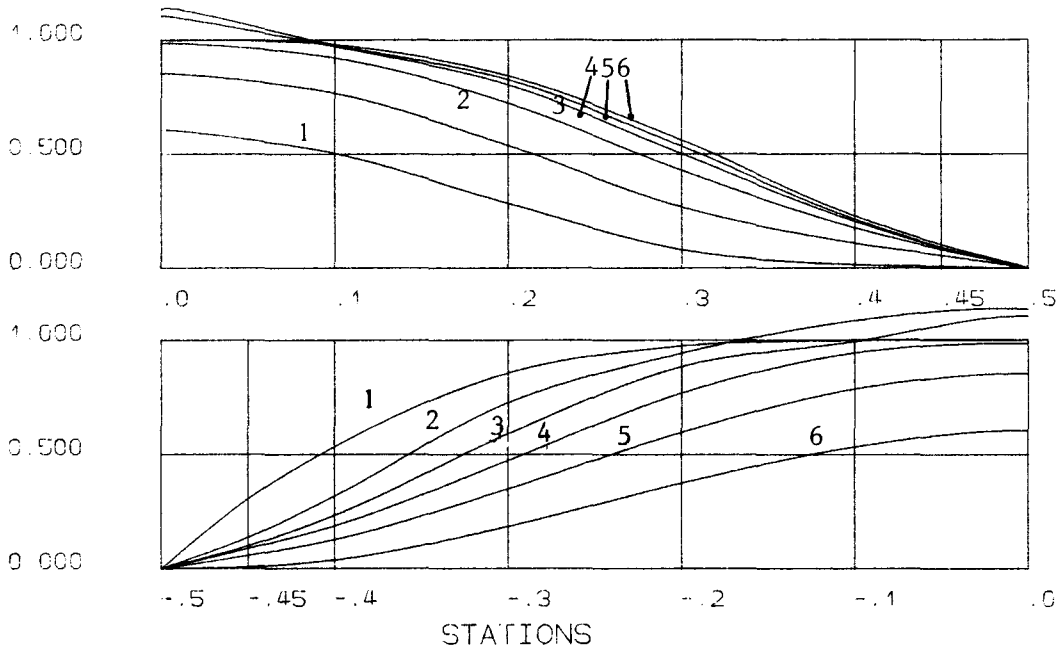
Table 2 Forebody offsets

j \ i	1	2	3	4	5	6	7
1	0.000	0.008	0.015	0.081	0.284	0.503	0.606
2	0.000	0.218	0.108	0.268	0.537	0.766	0.853
3	0.000	0.518	0.244	0.430	0.722	0.921	0.985
4	0.000	0.515	0.325	0.502	0.802	0.971	1.000
5	0.000	0.165	0.278	0.580	0.824	0.977	1.000
6	0.000	0.102	0.228	0.562	0.841	0.979	1.000

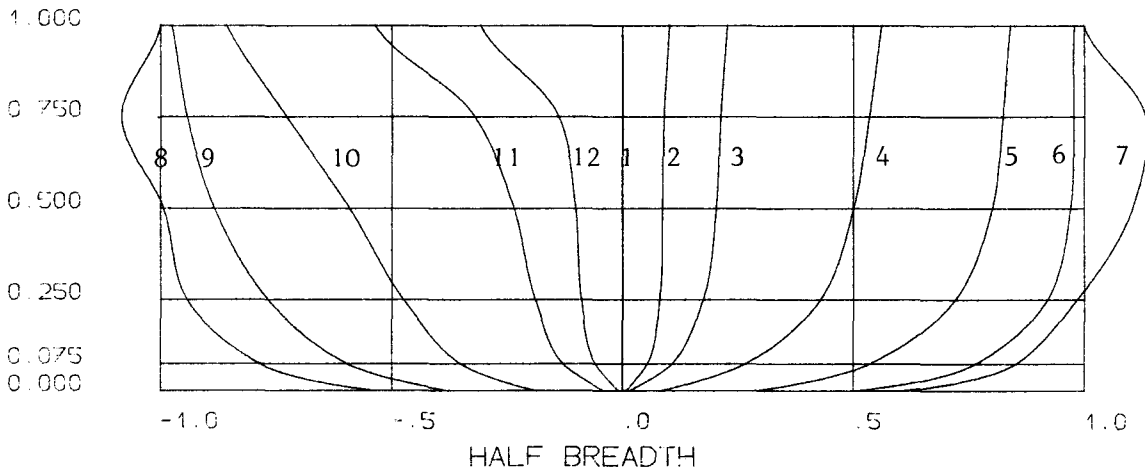
$F_n = 0.289, F_h = 0.945, q = 30$

$C_{to} = 1.548, C_t = 1.330, C_{fo} = 0.257, C_f = 0.267$ (with form factor correction)

WATER LINES



SECTION LINES



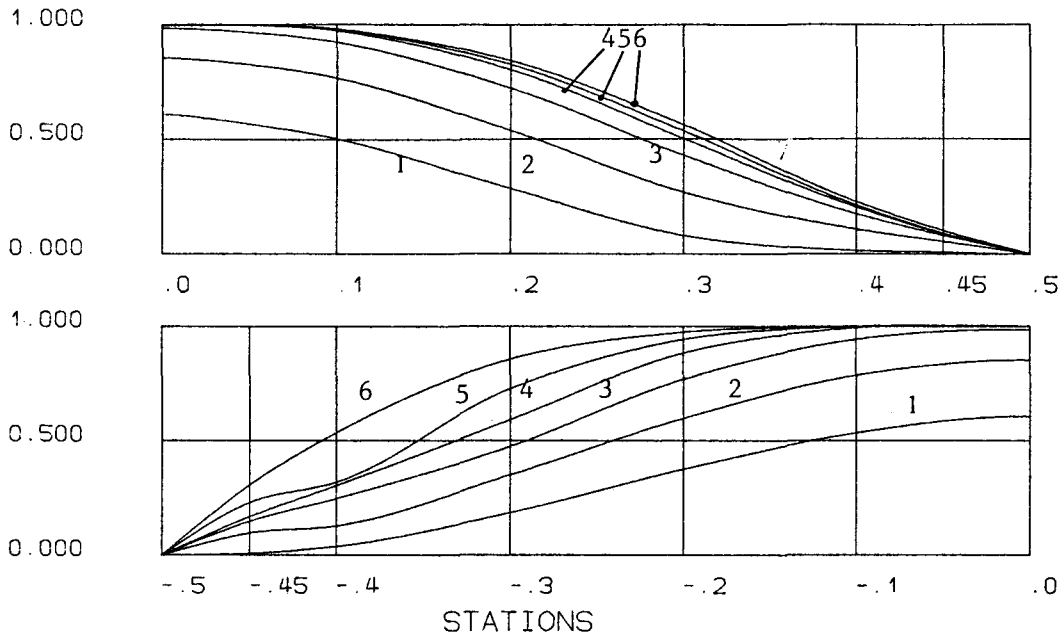
FN= 0.289 FH=0.000 Q= 30.

CTC =0.438 CT=0.386 DELTA=0.015

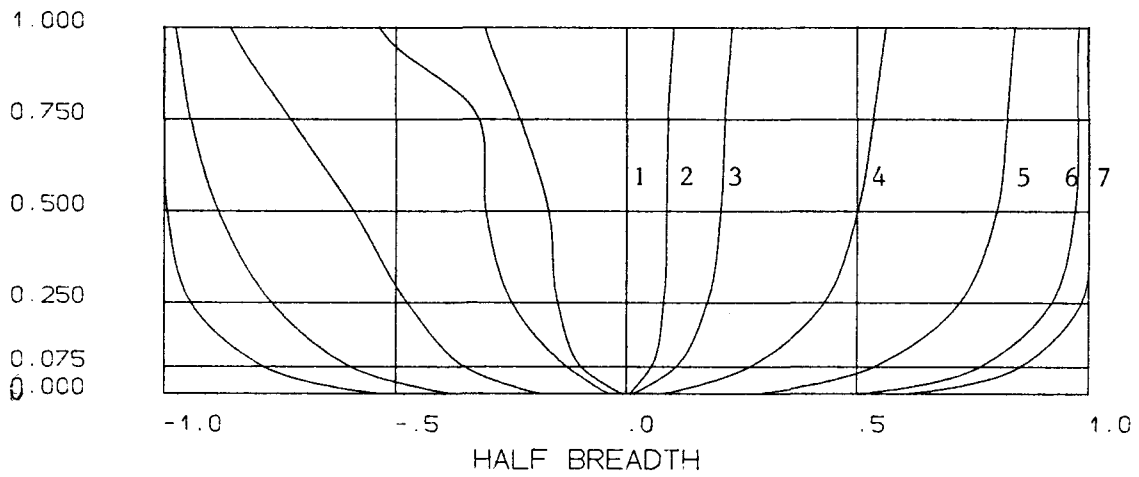
LR =2. AC=1.000 BO=1.200

Fig. 34

WATER LINES



SECTION LINES

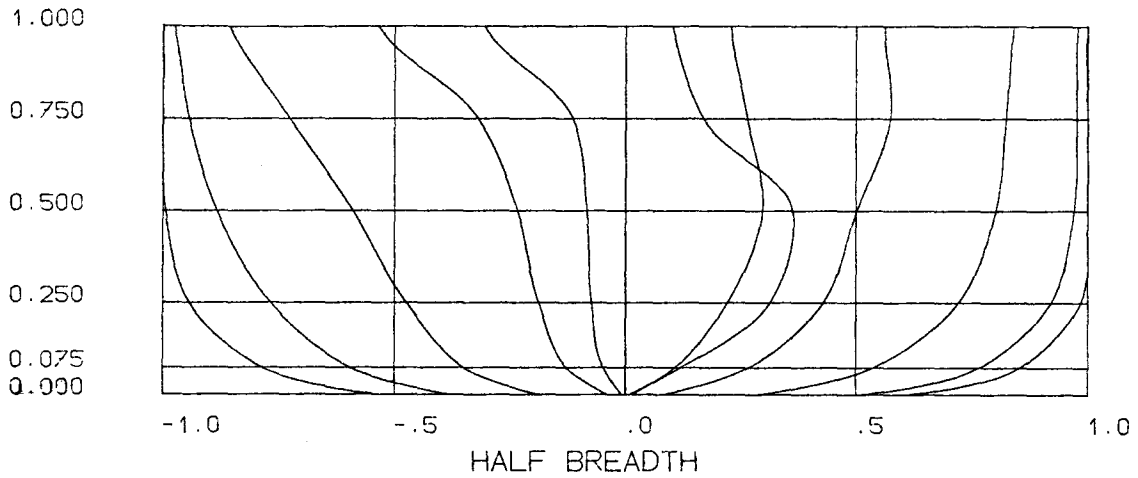


FN- 0.289 FH-0.919 Q- 30

CT0 -0.751 CT-0.692 DELTA-0.010

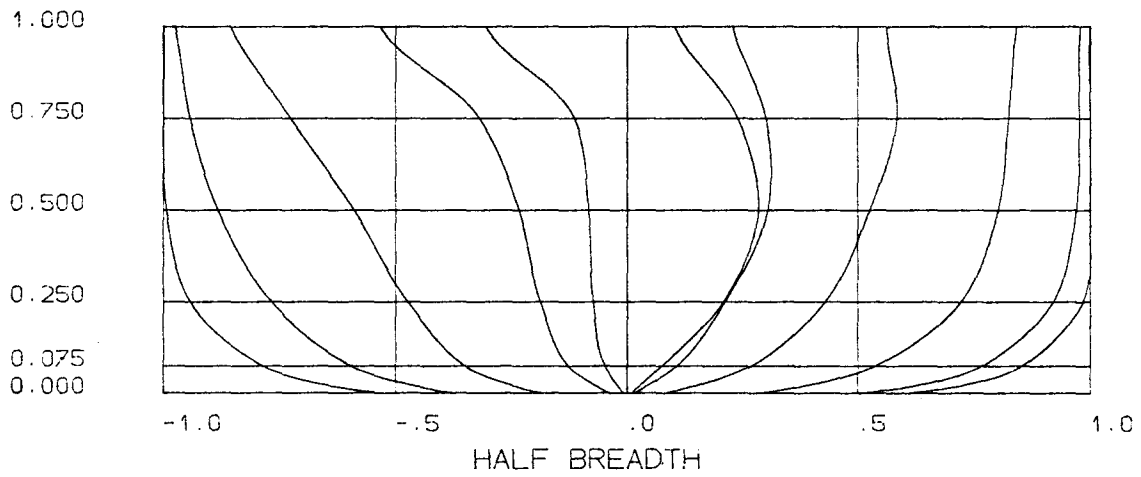
LR -2. A0-1.000 B0-2.000

Fig. 35



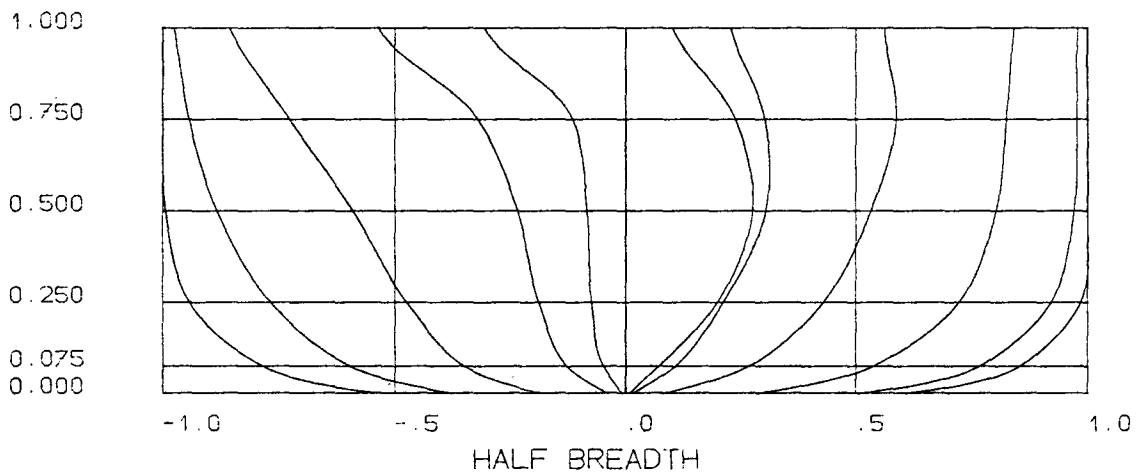
(a)

FN- 0.289 FH-0.919 Q- 25.000 VD=0.02 K=1



(b)

FN- 0.289 FH-0.919 Q- 25.000 VD=0.02 K=100



(c)

FN- 0.289 FH-0.919 Q- 25.000 VD=0.02 K=150

Fig. 36

CLOSING REMARKS

In the present study, an attempt was made to go in quest of shallow-water optimal ship forms for minimum total resistance by means of the quadratic-programming method under the constraints that the main dimensions of ship and water-plane area were kept constant. In fact, the present method can be used to calculate the optimal ship forms for minimum total resistance in arbitrary depth.

The great advantage of applying "tent" function to the optimization of ship forms is that one can directly obtain the reasonable non-negative solution of the optimal ship offsets rather than the optimal ship strut forms by which the ship lines can not be determined uniquely.

The wave-making resistance was calculated by Sretenski's formula and the viscous resistance was calculated by "1+k" method. Once a set of appropriate inequality-constraints is imposed, a practical, shallow-water optimal ship form for total resistance can be obtained by the quadratic programming method.

From the present study, the following conclusions were reached:

(1) There are obvious differences between deep-water and shallow-water optimal ship forms. Shallow-water optimal ship form will vary with depth Froude number F_h .

(2) Under the narrow-band constraints the optimization of shallow-water ship forms will generally lead to the ship forms with a larger prismatic coefficient and, by contrast, under the same conditions the optimization of deep-water ship forms will lead to the ship forms with a smaller prismatic coefficient.

(3) Although the frictional resistance was taken into account in a standard quadratic form, it does not guarantee against

no solution. In a great many of cases it will improve the solution suitability.

(4) Since the frictional resistance coefficient is a function of Reynolds number, the model scale will make a difference of the optimum ship form for total resistance. The smaller the model scale is, the greater the frictional resistance effect on the optimal ship form will be. However, the role of frictional resistance in damping wild behavior of optimal ship form is limited.

(5) If the damping role of frictional resistance is artificially augmented, the more practical optimal ship form can be obtained so that the present method of optimization ship forms can be used in the Computer Aided Hull Form Design.

ACKNOWLEDGEMENT

This work was performed under financial support from the DFVLR (Deutsche Forschungs- und Versuchsanstalt für Luft- und Raumfahrt).

The author wishes to express his deep gratitude to Prof. K. Eggers for his valuable suggestions and enthusiastic guidance.

Thanks are also extended to Prof. C.C. Hsiung for his encouraging discussion during his staying in Hamburg to attend the conference of 15 ONR-Symposium.

Additionally, the author gratefully acknowledges the support provided by the computer station of Institut für Schiffbau of University of Hamburg and thanks Mrs. L.v.Maydell for her typing this report.

REFERENCES

- /1/ Hsiung, Chi-chao:
"Optimal Ship Forms for Minimum Wave Resistance",
Journal of Ship Research, Vol. 25, No. 2, pp. 95-116,
June 1981
- /2/ Wehausen, J.V. and E.V. Laitone:
"Surface Waves", Encyclopedia of physics, Vol. IX, pp. 581,
1960
- /3/ Webster, W.C. and J.V. Wehausen:
"Schiffe geringsten Wellenwiderstandes mit vorgeschrie-
benem Hinterschiff", Schiffstechnik, Vol. 9, pp. 62-68,
1962
- /4/ Saunders, H.E.:
"Hydrodynamics in Ship Design", Vol. I, pp. 306-311,
Chapter 18,22,35 and 45, 1957
- /5/ Chen, Kenneth Keh-ya:
"Measurement of Wave Resistance in Water of Finite Depth
by Wave-pattern Analysis", Technical Report of University
of California, Berkeley, March 1973
- /6/ Kirsch, Maria:
"Shallow-water and Channel Effects on Wave Resistance",
Journal of Ship Research, Vol. 10, pp. 164-181, Sept. 1966
- /7/ Hsiung, Chi-chao and Dong Shenyan:
"Optimal Ship Forms for Minimum total Resistance", Journal
of Ship Research, Vol. 28, No. 5, Sept. 1984
- /8/ Lemke, C.E.:
"On complementary Pivot Theory", Mathematics of the
Decision Sciences, Part I, pp. 95-114
- /9/ Graff, W., A. Kracht and G. Weinblum:
"Some Extensions of D.W. Taylor's Standard Series",
Transactions SNAME, Vol. 72, pp. 374-396; disc. 396-403, 1964
- /10/ Kostyukov, A.A.:
"Theory of Ship Waves and Wave Resistance", translated by
Max Oppenheimer jr., published by E.C.I., Iowa City, Iowa,
1968
- /11/ Zhao, Lian-en, Huang, De-bo and Zhu, Nian-chang:
"Calculation of Wave Resistance of High Speed Ships with
Transom Stern", Journal of Harbin Shipbuilding Engineering
Institute, Vol. 6, No. 2, 1983

- /12/ Zhao, Lian-en:
"Theory of Wave Resistance of Ships and its Application",
Lecture of Harbin Shipbuilding Engineering Institute,
October 1982
- /13/ Miyazawa, Masaru:
"Minimization of Total Resistance of a Surface-piercing
Vertical Strut", Nagasaki Experimental Tank, Mitsubishi
Heavy Industries, 1984
- /14/ Shanghai Ship Transport Science Research Institute:
Report "Series Experiments of Shallow-water Ship
Resistance", September 1980